



LUND UNIVERSITY

Tomosynthesis in pulmonary cystic fibrosis

Vult von Steyern, Kristina

2013

[Link to publication](#)

Citation for published version (APA):

Vult von Steyern, K. (2013). *Tomosynthesis in pulmonary cystic fibrosis*. [Doctoral Thesis (compilation), Diagnostic Radiology, (Lund)]. Diagnostic Radiology, (Lund).

Total number of authors:

1

General rights

Unless other specific re-use rights are stated the following general rights apply:

Copyright and moral rights for the publications made accessible in the public portal are retained by the authors and/or other copyright owners and it is a condition of accessing publications that users recognise and abide by the legal requirements associated with these rights.

- Users may download and print one copy of any publication from the public portal for the purpose of private study or research.
- You may not further distribute the material or use it for any profit-making activity or commercial gain
- You may freely distribute the URL identifying the publication in the public portal

Read more about Creative commons licenses: <https://creativecommons.org/licenses/>

Take down policy

If you believe that this document breaches copyright please contact us providing details, and we will remove access to the work immediately and investigate your claim.

LUND UNIVERSITY

PO Box 117
221 00 Lund
+46 46-222 00 00

Tomosynthesis in pulmonary cystic fibrosis

Kristina Vult von Steyern



LUND
UNIVERSITY

AKADEMISK AVHANDLING

som för avläggande av doktorexamen i medicinsk vetenskap
vid Medicinska fakulteten, Lunds Universitet,
kommer att offentligen försvaras i demonstrationsrum 10, plan 4, BFC, SUS Lund,
fredagen den 29 november 2013, kl 13.00

Organization LUND UNIVERSITY Department of Diagnostic Radiology Clinical Sciences Lund, Faculty of Medicine	Document name DOCTORAL DISSERTATION	
Author: Kristina Vult von Steyern	Date of issue November 29, 2013	
Title and subtitle: Tomosynthesis in pulmonary cystic fibrosis		
<p>Abstract: The aims of this thesis were to investigate whether chest tomosynthesis might be used in pulmonary cystic fibrosis, to design and validate a tomosynthesis scoring system, and to determine the effective dose from chest tomosynthesis in children.</p> <p>In a prospective study starting in 2008 clinical chest radiography or computed tomography (CT) were supplemented with a tomosynthesis examination of the lungs. Tomosynthesis findings were characterized in comparison with radiography and CT findings, and used to design a scoring system for tomosynthesis. Conversion factors for paediatric chest tomosynthesis were determined by Monte Carlo simulations and used to estimate the effective dose from the registered dose-area-product from the patient examinations included in the study.</p> <p>The typical imaging findings of pulmonary cystic fibrosis were much better depicted with tomosynthesis compared with radiography. Most pulmonary changes visualised with computed tomography could also be evaluated well with tomosynthesis. A dedicated tomosynthesis scoring system was designed and validated, and proved to be robust. Bronchiectasis and mucus plugging are the most specific pulmonary changes of cystic fibrosis, and were in a review of commonly used radiological scoring systems generally considered the most important scoring components.</p> <p>For chest tomosynthesis in children the conversion factor was considerably higher for young children than previously reported for adults. The conversion factor increased with increasing tube energy and filtration. The mean paediatric effective dose from posteroanterior chest tomosynthesis was 0.17 mSv, which is about 40 times less than recently reported effective doses from paediatric chest CT. Using the previously reported conversion factor for adults the paediatric effective dose was estimated to 0.11 mSv. Consequently, when using conversion factors not adapted to children for paediatric examinations, the radiation dose may be underestimated. Anteroposterior exposures should be avoided, as the effective dose is approximately three times higher than for posteroanterior exposures.</p> <p>In these studies tomosynthesis has been shown to be a valuable tool for monitoring pulmonary cystic fibrosis, as typical imaging findings of this lung disease are well depicted and the radiation dose is low. The dedicated scoring system may improve diagnostic precision. At our radiology department, tomosynthesis now has to a great extent replaced radiography in the follow-up of these patients. CT is only performed in selected cases. Further studies are planned to determine the roles of tomosynthesis and CT in the evaluation of cystic fibrosis lung disease.</p>		
Key words: Cystic fibrosis; Lung; Radiation dose; Radiography; Scoring methods; Tomography, spiral computed; Tomography; X-ray computed.		
Classification system and/or index terms (if any)		
Supplementary bibliographical information	Language: English	
ISSN and key title: 1652-8220 Tomosynthesis in pulmonary cystic fibrosis		ISBN 978-91-87449-94-9
Recipient's notes	Number of pages 142	Price
		Security classification

Signature _____ Date _____

Tomosynthesis in pulmonary cystic fibrosis

Kristina Vult von Steyern



LUND
UNIVERSITY

Department of Diagnostic Radiology,
Clinical Sciences Lund, Faculty of Medicine,
Lund University and Skåne University Hospital, Lund

2013

Cover picture: Section from a tomosynthesis examination of an eight-year-old boy with cystic fibrosis. (*Author's image.*)

Thesis for the degree of Doctor of Philosophy in Medical Science

Department of Diagnostic Radiology, Clinical Sciences Lund,
Faculty of Medicine, Lund University and Skåne University Hospital, Lund

Lund University, Faculty of Medicine, Doctoral Dissertation Series 2013:121

Copyright ©2013 Kristina Vult von Steyern

ISBN 978-91-87449-94-9

ISSN 1652-8220

Printed in Sweden by Media-Tryck, Lund 2013



CLIMATE
COMPENSATED
PAPER



REPA[®]
A part of FTI (the Packaging and
Newspaper Collection Service)

Contents

List of papers	1
Thesis at a glance	2
Abbreviations and technical terms used	5
Populärvetenskaplig sammanfattning	7
Acknowledgements	9
Introduction	11
Background	13
Cystic fibrosis	13
Pathogenesis	13
Diagnosis	14
Treatment	15
Imaging of pulmonary cystic fibrosis	15
Scoring systems	15
Tomosynthesis	17
Historical background	17
Technique	19
Estimation of risks from X-ray exposure	20
History and background	20
Effective dose	21
PCXMC software for Monte Carlo simulations	22
Conversion factors	23
Aims	25
Paper I	25
Paper II	25
Paper III	25
Paper IV	25
Paper V	25

Methods	27
Paper I–III	27
Imaging findings of pulmonary cystic fibrosis	27
Development of the tomosynthesis scoring system	27
Validation of the scoring system	28
Comparison of scoring systems for cystic fibrosis	31
Paper IV–V	32
Conversion factor determination	32
Effective dose determination in a paediatric patient population	33
Phantom examinations	33
Results	35
Paper I	35
Paper II	40
Paper III	44
Abnormalities scored and scoring areas	44
Scoring levels and calculations for the final score	46
Weighting of scoring components	47
Paper IV	49
Paper V	52
Effective dose determination in a paediatric patient population	52
Phantom examinations	54
General discussion	55
Imaging of pulmonary cystic fibrosis	55
Scoring of pulmonary cystic fibrosis	56
Effective dose from chest tomosynthesis	58
The role of tomosynthesis in the monitoring of cystic fibrosis	60
Conclusions	63
References	65

List of papers

This thesis is based on the following papers, which will be referred to in the text by their Roman numerals I–V. The complete papers are appended at the end of the thesis.

- I. K. Vult von Steyern, I. Björkman-Burtscher, M. Geijer
Tomosynthesis in pulmonary cystic fibrosis with comparison to radiography and computed tomography: a pictorial review
Insights into Imaging 2012, 3:81–89
- II. K. Vult von Steyern, I.M. Björkman-Burtscher, P. Höglund, G. Bozovic, M. Wiklund, M. Geijer
Description and validation of a scoring system for tomosynthesis in pulmonary cystic fibrosis
European Radiology 2012, 22:2718–2728
- III. K. Vult von Steyern, I.M. Björkman-Burtscher, M. Geijer
Radiography, tomosynthesis, CT, and MRI in the evaluation of pulmonary cystic fibrosis- an untangling review of the multitude of scoring systems
Insights into Imaging 2013; doi: 10.1007/s13244-013-0288-y
- IV. K. Vult von Steyern, I.M. Björkman-Burtscher, M. Geijer, L. Weber
Monte Carlo simulations of conversion factors for estimation of effective dose in paediatric chest tomosynthesis
Radiation Protection Dosimetry 2013; doi: 10.1093/rpd/nct142
- V. K. Vult von Steyern, I.M. Björkman-Burtscher, L. Weber, P. Höglund, M. Geijer
Effective dose from chest tomosynthesis in children
Radiation Protection Dosimetry 2013; doi: 10.1093/rpd/nct224

Thesis at a glance

	Paper I	Paper II
Aims	To illustrate chest imaging findings of cystic fibrosis using tomosynthesis, in comparison to radiography and CT.	To design and validate a scoring system for tomosynthesis in pulmonary cystic fibrosis.
Methods	135 tomosynthesis and 135 radiography examinations in 36 children (8-18 y) and 39 adults (19-59 y), and 12 CT examinations from the same study population were evaluated and compared.	Based on typical pulmonary changes seen with radiography, tomosynthesis and CT, a new scoring system for tomosynthesis was designed. Three radiologists independently scored 88 pairs of radiographs and tomosynthesis examinations of the chest, using the Brasfield score for radiography and the new score.
Results	Typical pulmonary changes in cystic fibrosis such as mucus plugging and bronchiectasis are shown in much better detail with tomosynthesis than with radiography.	1) Observer agreements for the tomosynthesis score were almost perfect for the total score and generally high for subscores. 2) Correlation between the tomosynthesis score and the Brasfield score was good. 3) Tomosynthesis generally reached a higher score in percentage of the maximum score.
Conclusions	Tomosynthesis has a low radiation dose and low cost compared with CT, and gives a superior visualisation of pulmonary cystic fibrosis changes compared with radiography.	Compared with radiography, tomosynthesis is more sensitive to cystic fibrosis changes. The new scoring system offers the possibility of more detailed and accurate scoring of disease severity.

AP= anteroposterior, CT= computed tomography, DAP= dose-area-product, PA=posteroanterior

Paper III	Paper IV	Paper V
To analyse and compare scoring systems for cystic fibrosis, with special reference to which scoring components are considered most important.	To determine conversion factors from DAP to effective dose for chest tomosynthesis in children.	To determine effective dose from chest tomosynthesis in children.
Four scoring systems for chest radiography, one for tomosynthesis, eight for CT, and one for MRI were compared regarding scoring components, areas, levels, calculations for the final score and weighting of each component in % of total score.	Using the computer software PCXMC 2.0, simulations were performed on modified phantoms for males and females aged 8–19 years, in the PA and AP projection, with energies 80–140 kV and copper filtration 0.1–0.3 mm.	74 children were examined with chest tomosynthesis, totally 169 PA and 17 AP examinations (mean age 13.7 years, range 7–20 years). The effective dose was calculated by multiplying DAP with conversion factors determined in Paper IV.
In most scoring systems the lungs are evaluated for increased volume, bronchial wall thickening, bronchiectasis, mucus plugging, atelectasis and consolidation. In addition, e.g. mosaic perfusion, ground glass opacities and air trapping are evaluated in some CT scoring systems and perfusion defects are scored on MRI.	Resulting conversion factors ranged between 0.23 and 1.09 mSv/Gycm ² , decreased with patient age, were significantly higher in the anteroposterior projection and increased with increased energy or copper filtration.	Using the conversion factors from Paper IV corrected for sex, age and energy (0.23–1.09 mSv/Gycm ²) the mean posteroanterior effective dose was 0.17 mSv and using the proposed simplified conversion 0.15 mSv. AP exposures had considerably higher effective dose.
Bronchiectasis alone, or in combination with mucus plugging, is given the highest weighting in most scoring systems and is thus commonly considered to be the most significant finding when evaluating cystic fibrosis lung disease.	To avoid an underestimation of effective dose in children it is recommended to use age dependent conversion factors. As a simplified approach three conversion factors might be used for PA chest tomosynthesis in children, namely 0.6 (8–10 years), 0.4 (11–14 years) and 0.3 mSv/Gycm ² (15–19 years).	It is recommendable to use the simplified conversion factors. By using conversion factors adapted to children the calculated risks from radiologic procedures will be more accurate.

Abbreviations and technical terms used

AP	Anteroposterior
Conversion factor	E_{DAP} (in mSv/Gycm ²). By multiplying DAP (in Gycm ²) with a conversion factor the effective dose (in mSv) can be calculated. The conversion factor depends on the type of examination, exposure settings and patient size.
Cu	Copper
CT	Computed tomography
DAP	Dose-area-product (mGycm ²). The surface area of the patient that is exposed to radiation at the skin entrance (in cm ²) multiplied by the radiation dose at this surface (in mGy). In the X-ray system used in these studies DAP was automatically registered.
Effective dose	E (in mSv). The purpose of effective dose calculations is to estimate the risk for the entire body from exposure of a part of the body. Effective dose is the sum of the radiation doses delivered to each organ multiplied by the organs tissue weighting factor. It can be calculated by multiplying DAP with a specific conversion factor.
ICRP	International Commission on Radiological Protection
kV	Kilovolt (tube voltage or energy)
mAs	Milliampere second (tube load)
MRI	Magnetic resonance imaging
PA	Posteroanterior
Scout image	In the equipment used in this thesis a tomosynthesis examination always includes a scout image, which is a PA or AP radiograph, which is used by the system for determining the tube load for the tomosynthesis acquisitions.

SD	Standard deviation
Tissue weighting factor	Carcinogenic sensitivity of organs and tissues differ, therefore the relative contribution of each organ or tissue to the total health detriment from uniform irradiation of the body is weighted. The sum of all tissue weighting factors is 1.
Tomosynthesis	Digital tomography. In the equipment used in this thesis a tomosynthesis examination includes a scout image, which is a PA or AP radiograph, and the tomosynthesis acquisition.

Populärvetenskaplig sammanfattning

Tack vare den snabba tekniska och digitala utvecklingen under senare år har tomosyntes etablerats som ett nytt och spännande verktyg inom röntgendiagnostiken. Metoden är en vidareutveckling av gammaldags tomografi (skikt-röntgen), men är lättare att utföra, ger bättre bilder och dessutom är stråldosen betydligt lägre.

Vid tomosyntes gör röntgenröret ett svep över den kroppsdel som ska undersökas och samtidigt bestrålas detta område. Bakom patienten finns en detektor som samlar informationen, som sedan bearbetas i en dator. När man gör tomosyntes av lungor blir slutresultatet ca 60 skiktbilder av lungorna, med 3–4 mm avstånd mellan varje skikt. Bilden liknar vanlig lung-röntgen, men skillnaden är att strukturer i bildskiktet är skarpt avbildade och strukturer framför eller bakom blir utsuddade och oskarpa.

Våren 2008 installerades tomosyntes på vår röntgenavdelning. Eftersom luftvägarna och förändringar i lungvävnaden avbildas tydligt med tomosyntes insåg vi att metoden kunde lämpa sig för att följa patienter med cystisk fibros. Detta är en medfödd, obotlig sjukdom där tjockt slem bildas bland annat i luftvägarna. Patienterna har svårt att hosta upp slemmet vilket leder till inflammation och infektion i luftvägarna, som svullnar och efterhand utvidgas. Tidigare har patienter med cystisk fibros följts med lung-röntgen och ibland även med datortomografi. I studien kompletterades dessa undersökningar med tomosyntes av lungorna.

Syftet med den *första delstudien* var att kartlägga hur förändringar i lungorna vid cystisk fibros avbildas med tomosyntes jämfört med lung-röntgen och datortomografi. I materialet ingick då 135 tomosyntes- och lung-röntgenundersökningar (från 36 barn och 39 vuxna) och 12 datortomografiundersökningar. Tomosyntes visade de förändringar som är typiska för cystisk fibros, slempluggar i luftvägar och förtjockade och utvidgade luftvägar, mycket tydligare jämfört med lung-röntgen. Merparten av förändringarna som sågs på datortomografi var väl framställda även med tomosyntes.

I den *andra delstudien* utvecklades ett s.k. scoringsystem för tomosyntes. Detta för att kunna skatta (poängsätta) graden av förändringar vid cystisk fibros. Syftet med poängsättningen var att på ett mer objektivt sätt kunna följa sjukdomsutvecklingen och effekten av olika behandlingsstrategier. Det nya scoringsystemet beskrevs i detalj och användes på 88 tomosyntesundersökningar av barn och vuxna med cystisk fibros. Detta jämfördes sedan med lung-röntgenundersökningar från samma tidpunkt, som skattades med en vedertagen lung-röntgen score, s.k. Brasfield score. Scoringsystemet

för tomosyntes visade sig fungera väl, med god överensstämmelse mellan bedömare och med skattningen av lungröntgen. Tomosyntes var, som förväntat, en känsligare metod än lungröntgen för att påvisa cystisk fibros förändringar i lungorna.

I den *tredje delstudien* jämfördes hur cystisk fibros förändringar kan skattas på lungröntgen, tomosyntes, datortomografi och magnetkameraundersökningar. De mest använda scoringsystemen för de olika metoderna jämfördes avseende likheter och olikheter. Scoringen utförs på mycket olika sätt i de olika systemen. I nästan alla scoringsystem skattas dock lungorna för graden av ökad lungvolym, slempluggar, förtjockning av luftvägar, utvidgning av luftvägar och förtätning av lungvävnad. Det viktigaste fyndet i majoriteten av scoringsystemen var utvidgade luftvägar, eventuellt i kombination med slempluggar.

Eftersom barn med cystisk fibros kommer att genomgå många röntgenundersökningar under sin livstid är det viktigt att veta vilken stråldos undersökningarna ger, och om möjligt välja undersökningar med låg stråldos. I röntgenapparaten registreras automatiskt en s.k. dose-area-product (DAP), vilket är stråldosen vid hudytan multiplicerat med storleken på den bestrålade hudytan. För att kunna omvandla DAP till ett mått på risken med bestrålningen (s.k. effektiv dos, anges i mSv) multipliceras värdet med en s.k. konversionsfaktor (omvandlingsfaktor).

Syftet med den *fjärde delstudien* var att ta fram konversionsfaktorer för tomosyntes av lungor på barn. Med hjälp av datorprogrammet PCXMC 2.0, utvecklat av finska strålskyddsmyndigheten STUK, kan man beräkna stråldoser och konversionsfaktorer genom simulerade röntgenundersökningar. Undersökningar både i stående och liggande simulerades för flickor och pojkar från 8 till 19 år. Konversionsfaktorerna minskade med stigande ålder, ökade med stigande rörspänning (energi) eller filtrering, och var högre vid undersökning i liggande än i stående. För de minsta barnen var konversionsfaktorerna betydligt högre än faktorn som tidigare rapporterats för vuxna. För att korrekt beräkna riskerna för barn med bestrålning är det därför viktigt att använda konversionsfaktorer anpassade till barn.

I den *femte delstudien* användes de konversionsfaktorer vi hade uppmätt i delstudie fyra för att beräkna vilken effektiv dos tomosyntes av lungor ger till barn. Här ingick 186 undersökningar på barn i åldrarna 7 till 20 år. Den beräknade medeldosen uppgick till 0,17 mSv, vilket är högre än den dos på 0,12–0,13 mSv som tidigare rapporterats för vuxna, men bara ca 1/40 av nyligen rapporterade doser för datortomografi av lungor på barn. Medelstråldosen för liggande undersökning var ca 3 gånger högre än för stående undersökning.

Tomosyntes har visats vara ett värdefullt verktyg i uppföljningen av patienter med cystisk fibros. De typiska lungförändringarna vid cystisk fibros avbildas väl med metoden och stråldosen är låg. Vidare studier är planerade för att ytterligare kartlägga vilken roll tomosyntes och datortomografi bör ha i uppföljningen av dessa patienter.

Acknowledgements

First of all I would like to thank Wilhelm Conrad Röntgen for discovering X-rays, and all researchers who participated in the development of tomosynthesis. Without their work this thesis project would not have been possible, and I would be doing something completely different.

Accomplishing a doctoral thesis is a long and laborious process, but thanks to support and encouragement from colleagues, friends and family this has been a fulfilling, and actually, a quite pleasant experience. I would especially like to thank:

Isabella Björkman-Burtscher, for sensible advice and teaching me how to structure my research and writing.

Mats Geijer, for always giving prompt answers, well thought-out advice and point-of-views, both on my research and on life in general.

Peter Hochbergs and Pia Maly Sundgren, for making it possible to perform research at our department and for giving me the time required.

Ingvar Kristiansson and Ina Kehler, for encouraging research at Röntgen 2.

Pär Wingren, for supporting me in my research, and making it possible for me to have time-off from the clinical work to pursue my research. And, not least, for assisting in the development of the tomosynthesis scoring system.

Region Skåne, for financial support.

Gracijela Bozovic, for your valuable in-put in the design of the scoring system and your perseverance in scoring the examinations, as well as for fruitful discussions over white wine and sushi.

Peter Höglund, for elucidating the jungle of statistics and, as by magic, transforming numbers into comprehensible results and figures.

Lars Weber, for explaining the mysteries of radiation physics, guiding me through the PCXMC software and helping me with figures.

Marie Wiklund, my friend, colleague, room mate and travel partner. For your devotion in all my projects and your enthusiasm at scoring examinations. And, not least, for all our exciting trips together, and for being my friend and support.

All staff and technicians at Röntgen 2, for your optimism and competence, and especially Agne, Ali, Anki, Annika, Carina, Ione, Jennie and Maria for performing phantom examinations.

Carina Fyledahl-Kastberg, for keeping the patient log and for performing a multitude of tomosynthesis examinations.

Gerhard Brunst, for answering my questions about tomosynthesis and giving constructive criticism on the section on tomosynthesis technique in this thesis.

My colleagues Pär, Marie, Sofie, Fredrik, Lotta and Lisa at the Paediatric Radiology Department, for supporting me and holding the fort when I haven't been there.

All my workmates, for making it a pleasure going to work in the morning.

Inger Bjarke, for your never-ending enthusiasm, for great PACS support when I was in despair and for anonymising the studies.

Karin Jönsson and Annika Törling-Ring, for helping me with administrative issues.

Åsa Schiött, for being my friend since almost forever.

Pia Hansson, for great conversations over a glass of red wine.

The Pulverer family, for skiing trips to Bad Klein Kirchheim, tennis tournaments on Ramsvik, long dinners and marvellous parties.

The Frenander family, for boat trips, dinners at sunset on small islands of the West Coast archipelago, and for evenings with lots of laughter playing party games.

My mother-in-law Bettan, for your wisdom and zest for life.

My big sister Cecilia, for long telephone conversations about small and big things, for supporting me and for always being proud of me.

My father Jan and my mother Gudrun, for persuading me not to quit after the first week of Medical School, for inspiring me and for supporting me all these years.

Bruno, my Jack Russell terrier, for unconditional love and great company on long walks, helping me clear my mind.

My children Hanna, Karl and Emma, for all happiness that you have brought to me and for reminding me what really is important. I am unspeakably proud of you all.

Fredrik, for accompanying me on my journey and for all wonderful experiences that we have had together, with hope of many good years to come.

Introduction

Children are more sensitive to radiation and have a longer presumed life span than adults, thus their lifetime risk for radiation induced malignant disease is higher⁽¹⁻³⁾. With improved treatment regimes patients with cystic fibrosis are expected to live longer⁽⁴⁾ and during their lifetime they will be exposed to significant radiation doses from medical imaging. According to the ALARA principle (As Low As Reasonably Achievable)⁽⁵⁾ it is therefore important to use, if possible, imaging modalities with low or no radiation.

In the monitoring of pulmonary cystic fibrosis chest radiography has been the mainstay of imaging modalities. It is easily accessible, has low cost and low radiation dose. Computed tomography (CT) of the chest is generally considered as the “gold standard”, but as the effective dose from CT is high⁽⁶⁾ it is important to consider using alternative methods with less radiation⁽⁷⁾. The annual effective dose *per capita* from radiologic examinations has increased in the last decades, worldwide it has approximately doubled in the past 10-15 years⁽⁸⁾. In Norway the frequency of chest X-ray examinations has been reduced with about 20% from 1993 to 2002. In the same time period the frequency of chest CT examinations has increased with 304%⁽⁹⁾. In Norway the annual effective dose *per capita* from radiologic examinations was 1.09 mSv in 2002 (a 40% increase from 1993), and CT was estimated to account for 59% of the total dose. This dose is comparable with the annual dose from natural background radiation, which is about 1 mSv in Sweden⁽¹⁰⁾.

In 2008 the X-ray system at our department was supplemented with tomosynthesis. Tomosynthesis had by then been used for mammography for more than a decade, and technical developments now had led to the introduction of the technique for chest⁽¹¹⁻¹³⁾, abdominal^(14, 15) and musculoskeletal^(16, 17) imaging. In chest tomosynthesis a single low-dose acquisition can generate multiple coronal image planes of the lungs. Objects in the focus plane are sharp and objects located out of the focus plane are blurred.

The aims of this thesis were to investigate whether tomosynthesis could be used in the follow-up of patients with cystic fibrosis, to design and validate a chest tomosynthesis scoring system, and to determine the effective dose from chest tomosynthesis in children.

Background

Cystic fibrosis

Pathogenesis

Cystic fibrosis was first described in 1938⁽¹⁸⁾ following autopsy studies of malnourished infants, in whom extensive mucus plugging of the airways and in the pancreas was found. The children had a clinical history of lung infections and poor growth⁽¹⁹⁾. The underlying defect in chloride transportation was identified in 1983⁽²⁰⁾. In 1989 it was discovered that cystic fibrosis is an autosomal recessive inherited disorder, caused by a gene defect on chromosome 7 coding for the cystic fibrosis transmembrane regulator (CFTR)⁽²¹⁾ protein. The defect causes abnormal ion transfer across the epithelium, with failure to excrete chloride and an increased reabsorption of sodium⁽¹⁹⁾. This leads to excessive absorption of fluid, the mucus becomes dehydrated and hyperviscous, and cilia activity is inhibited⁽²²⁾. This causes problems mainly in the lungs and the gastrointestinal tract and results in respiratory distress, lung infections and poor absorption of nutrients. Another sign is unusually salty sweat⁽⁴⁾. In Sweden approximately 20 children annually are born with cystic fibrosis. In the whole country there are currently about 650 people affected by the disease⁽⁴⁾. The first sign of the disease may be meconium ileus, when thick faeces obstructs the bowel in neonates with cystic fibrosis. Most children affected by the disease have frequent respiratory infections and a stubborn cough⁽⁴⁾.

In the lungs mucociliary clearance and mucosal defence against bacteria are impaired. Bacteria persist in the airways and produce epithelium-damaging substances⁽²³⁾. In addition the CFTR protein regulates the airway surface liquid depth⁽²⁴⁾ and defects in CFTR are also associated with increased production of proinflammatory mediators⁽²⁵⁾. Furthermore, it has been implied that the CFTR protein abnormality can lead to increased bacterial adhesion to the cell surface⁽²⁶⁾.

The lungs of children with cystic fibrosis are essentially normal at birth⁽²⁷⁾, but early in life they are prone to bacterial infection⁽²⁸⁾. The bacteria in the airways trigger an inflammatory response which further damages the airways, resulting in a “vicious circle”^(23, 29) of infection, impaired mucociliary clearance, inflammation, bronchial

obstruction⁽²²⁾ and tissue damage. Some authors have suggested that inflammation even may precede infection⁽³⁰⁾. Eventually permanent bacterial colonization of the airways will be established, with pathogens such as *Haemophilus Influenzae*, *Staphylococcus aureus* and *Pseudomonas aeruginosa*.

The airway walls are gradually destroyed by infection and inflammation. The small airways are reduced in size due to inflammation and squamous metaplasia, leading to airway obstruction⁽²²⁾. The bronchial walls are thickened. The glands and secretory cells in the epithelium increase in volume, which leads to excessive mucus production and airway impaction^(22, 28) and bronchiectasis ensues. Initially the bronchiectasis is cylindrical but as the disease progresses the bronchi successively become more dilated, varicose, and finally cystic, the most severe form of bronchiectasis^(31, 32).

The course of the disease is thus chronic progressive. The general state of health of those affected with the disease deteriorates gradually, but there are large variations in the severity of symptoms. Certain individuals with cystic fibrosis do not show clear symptoms until they reach adulthood. In the past, most children did not survive childhood, but in Sweden the average life expectancy is currently approximately 50 years of age and is expected to rise further in line with medical advances⁽⁴⁾.

Diagnosis

The diagnosis of cystic fibrosis is based on DNA tests, or on two sweat chloride tests where both reveal abnormally high levels of chloride ions, combined with other symptoms of the disease⁽⁴⁾. The sweat test remains the “gold standard” for cystic fibrosis diagnosis, but does not always give the diagnosis⁽³³⁾ as in a few per cent of cases levels may be normal⁽⁴⁾. There are individuals with classic symptoms of the disease who, despite extensive DNA analysis, cannot be shown to have any known mutation to their CFTR-gene⁽⁴⁾. More than 1500 mutations have been identified in the gene, not all of which result in cystic fibrosis⁽³³⁾. Prenatal testing is possible if genetic mutations are known in a family and new-born screening for cystic fibrosis is increasingly being implemented⁽³³⁾, identifying high levels of immunoreactive trypsinogen in the blood of newborns at risk for cystic fibrosis. Ultrasound has also been used to detect cystic fibrosis *in utero*, as the finding of an echogenic bowel in the foetus implies an increased risk of cystic fibrosis⁽³⁴⁾. In the United States the median age at diagnosis is 6 months, and mean age at diagnosis is 3 years⁽³⁵⁾. When children are affected by meconium ileus the diagnosis is often made earlier.

Treatment

The therapies for cystic fibrosis have improved dramatically in the past decades, offering the promise of an improved general state of health and increased life expectancy. Efforts to clear excessive, hyperviscous mucus with expectorants and breathing exercises, and physical training represent the basis of cystic fibrosis therapy^(4, 36). Early and aggressive treatment of pulmonary infections is important, and is believed to be the main reason for the reduced morbidity in cystic fibrosis over the past decades^(36, 37), as well as vaccinations⁽⁴⁾. Anti-inflammatory drugs have also shown to be beneficial in cystic fibrosis⁽³⁶⁾, but are not yet commonly used due to side effects. In addition, on-going studies aim to find treatments intended to normalise the defect ion transport and to restore the function to the mutant CFTR protein⁽³⁶⁾. For patients with severe lung disease lung transplantation may become necessary⁽⁴⁾.

Imaging of pulmonary cystic fibrosis

Typical chest imaging features of cystic fibrosis are overinflation, bronchial wall thickening, bronchiectasis, mucus plugging, atelectasis and consolidation. In addition abscesses, cysts, bullae, thickened intra- or interlobular septa, mosaic perfusion, ground-glass opacities and air trapping can be evaluated with CT. Perfusion defects can be evaluated with contrast enhanced MRI.

Radiography is often used to follow the development of pulmonary changes in cystic fibrosis, and to detect complications of the disease. CT is the “gold standard” due to the combination of high contrast resolution and detailed spatial resolution. The role of CT is, however, under investigation⁽³⁸⁻⁴⁰⁾. CT has up to now mainly been used for research purposes, due to the comparatively high radiation dose⁽⁶⁾. Therefore, tomosynthesis^(41, 42) and MRI⁽⁴³⁻⁴⁶⁾ have recently appeared as alternatives to CT for more detailed evaluation of cystic fibrosis of the lungs compared with radiography.

Scoring systems

The first radiography scoring system for pulmonary cystic fibrosis was described in 1958, by Shwachman and Kulczycki⁽⁴⁷⁾. This is a clinical evaluation score, and radiographic findings are evaluated together with general activity, physical examination and nutrition. Since then a multitude of chest radiography scoring systems have been presented, where some are parts of clinical scores^(48, 49) and others are pure radiographic scores⁽⁵⁰⁻⁵⁸⁾.

In 1974 the first dedicated chest radiography score was presented by Chrispin and Norman⁽⁵⁰⁾. In this system examinations are evaluated for chest configuration and four lung quadrants are evaluated for bronchial line shadows, mottled shadows, ring shadows and large pulmonary shadows. The Brasfield scoring system⁽⁵¹⁾, which is used at the department of paediatric radiology in Lund, was introduced in 1979. This scoring system is similar to the Chrispin-Norman score⁽⁵⁰⁾, but the nomenclature differs and both lungs are evaluated together for air trapping, linear markings, nodular-cystic lesions, large lesions and general severity. In a study by Terheggen-Lagro *et al.* from 2003⁽⁵⁹⁾, six chest radiography scoring systems^(47, 50-52, 55, 56) were compared. The authors preferred the Chrispin-Norman score⁽⁵⁰⁾, since it was simple, but concluded that all compared scoring systems showed low intraobserver variability and correlated well with lung function tests and infectious exacerbation rate. The Northern score⁽⁵⁶⁾, presented in 1994, was recommended for use by the authors of a European consensus paper on standards of care for patients with cystic fibrosis in 2005⁽⁶⁰⁾. The Northern score has the advantage of only requiring the frontal radiograph for scoring, while most other scoring systems use both the frontal and lateral radiograph.

CT and the mathematical algorithms necessary were presented by Hounsfield⁽⁶¹⁾ and Cormack⁽⁶²⁾, respectively, and they were awarded the Nobel Prize in medicine in 1979. The first clinical CT prototype was installed in 1972. In 1991 the first cystic fibrosis scoring systems for CT were presented, by Nathanson *et al.*⁽⁶³⁾ and Bhalla *et al.*⁽⁶⁴⁾. In the Nathanson score only bronchiectasis and mucus plugging are evaluated. In the Bhalla score the lungs are evaluated for bronchiectasis, peribronchial thickening, mucus plugging, sacculations or abscesses, bullae, emphysema, and collapse or consolidation. Since then a plethora of scoring systems for CT has been presented⁽⁶⁵⁻⁷⁶⁾, using different scoring parameters and scoring approaches. In some scoring systems^(69, 73, 75) expiratory scans are included and air trapping can be evaluated.

The first cystic fibrosis scoring system for MRI was presented in 2012 by Eichinger *et al.*⁽⁴⁶⁾. As the MRI examinations for this score are performed using intravenous contrast, lung perfusion can be evaluated. In addition, the lungs are scored for bronchiectasis and wall thickening (entities that cannot be separated by MRI), mucus plugging, abscess and sacculaton, consolidation and pleural affection (reflecting for example pleural effusion or pneumothorax). When the present thesis project started no scoring system for tomosynthesis had yet been published.

Tomosynthesis

Historical background

Tomosynthesis originates from the Greek words *tomo* (cut or slice) and *synthesis* (the combining of separate parts to form a complex whole). The term was coined by Grant in 1972⁽⁷⁷⁾, but the mathematical principle behind tomosynthesis (the shift-and-add technique, Fig. 1) goes back to the works of Radon in 1917⁽⁷⁸⁾. Radon⁽⁷⁸⁾ created a mathematical formula for tomography by which projection data through an object could be used to reproduce the inner structure of a body.

Tomosynthesis is a development from conventional geometric tomography, described by Ziedses the Plantes⁽⁷⁹⁾ in 1932. A plane of interest is produced by moving the detector (originally screen-film) and the X-ray tube in opposite directions across the patient. Structures located within the plane about which the tube and detector move are sharp, and those located outside the plane of interest are blurred. The tomographic technique provides depth localisation, enables removal of overlying disturbing anatomy, such as ribs, and improves the contrast of the structures in plane. The drawback with this method is that only a single plane can be acquired at a time, which makes the examination of a whole volume time consuming and at the price of a high radiation dose⁽⁸⁰⁾. Therefore, geometric tomography was gradually replaced by CT and MRI.

In tomosynthesis many tomographic scans are generated from a single low-dose acquisition procedure. The technique was gradually developed and improved in the 1960s and 1970s. But it was not until the late 1990s, with the introduction of flat-panel detectors, improved artefact reducing algorithms and increasing computer speed that the technique was clinically practical⁽⁸¹⁾. The flat-panel detectors enable rapid image acquisition with few artefacts, which is crucial for tomosynthesis examinations.

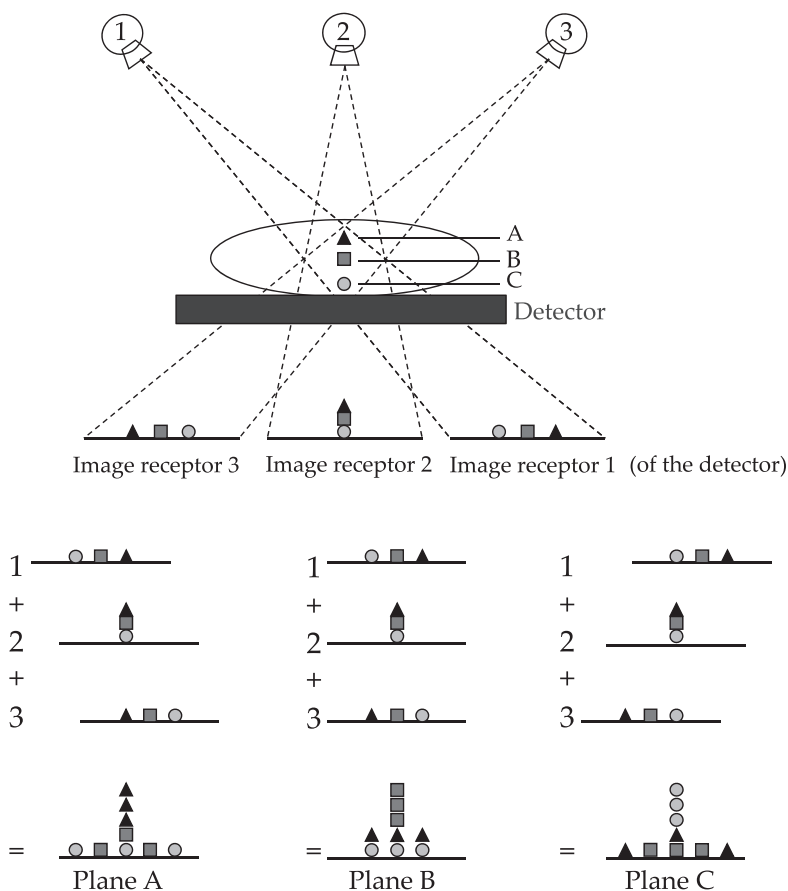


Fig. 1

Schematic illustration of the shift-and-add technique. In this example an X-ray tube moves to three different positions, with different projection angles in relation to the objects A (*triangle*), B (*square*) and C (*circle*). At the different projection angles objects in Plane A, Plane B and Plane C are projected at different locations in the image receptors 1, 2 and 3 of the detector. The three projection images are then shifted and added together, yielding a summation image. Depending on the magnitude of the shift planes at different depths are in focus. In this example object A is sharp in Plane A, but objects B and C (which are located outside the image plane) are blurred, but can sometimes generate out-of-plane artefacts depending on the size and contrast of the object. In Plane B object B is in focus and in Plane C object C. (Courtesy of Angelica Svalkvist, Dept. of Radiation Physics, University of Gothenburg. Adapted with permission.)

Technique

In tomosynthesis a single low-dose acquisition can generate an arbitrary number of in-focus image planes throughout the entire volume of interest. Objects in the focus plane are sharp and objects located outside the focus plane gradually fade out; how far away from the focus plane objects are visible depends on the size and the contrast of the object. Therefore, high contrast objects such as central venous access devices and side markers can generate so called out-of-plane artefacts.

In the digital linear tomography system used for chest tomosynthesis in this study (Definium 8000 with VolumeRAD option; GE Healthcare, Chalfont St Giles, UK) the X-ray tube moves in a linear path from -17.5° to $+17.5^\circ$, while radiation exposure and data collection is active from -15° to $+15^\circ$. During this sweep multiple low-dose exposures are directed towards a stationary digital amorphous flat panel detector (Fig. 2). The generated 60 projection images are used to automatically reconstruct approximately 60 coronal tomosynthesis sectional images in a work station, with a focus plane distance of 3 mm for children and 4 mm for adults, using filtered back-projection (which is an advanced form of the shift-and-add technique) (Fig. 1).

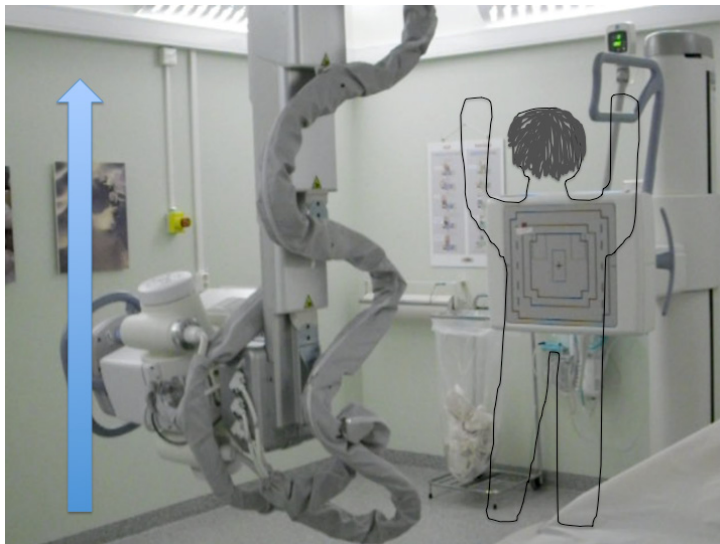


Fig. 2

The tomosynthesis system used at the Paediatric Radiology Dept. at Skåne University Hospital in Lund. The patient (*schematically drawn in grey*) is positioned close to and facing the flat panel detector. A motorized tube crane allows the X-ray tube to move in a linear vertical path (*blue arrow*), while rapidly acquiring multiple low-dose projection images from different tube angles of the area of interest. (*Author's image.*)

The tube movement in chest tomosynthesis takes about 10 s, and requires a breath held in deep inspiration. Thus, small children may have problems cooperating for the examination. The examination can usually be performed successfully in children from about eight years old. The tube crane in the system, which moves the tube during the examination, can be used for both a vertically mounted wall stand and a horizontal tabletop, enabling examinations in standing (PA) or supine position on the examination table (AP).

Estimation of risks from X-ray exposure

History and background

In 1895 Wilhelm Conrad Röntgen discovered X-rays, and one of the first radiographs produced was of his wife Bertha's hand (Fig. 3). Röntgen was awarded the first Nobel Prize in physics in 1901.

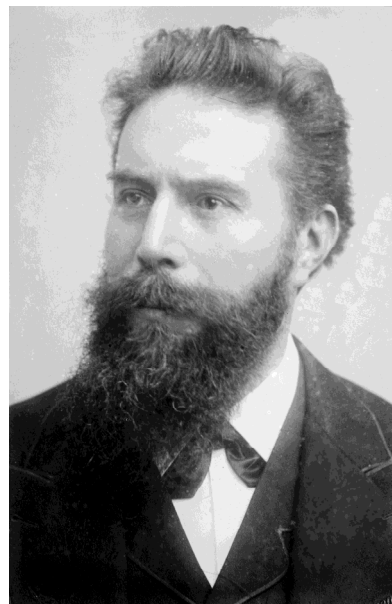


Fig. 3
Hand mit Ringen (Hand with Rings) (**left**): one of the first medical X-ray images by Wilhelm Conrad Röntgen (1845–1923) (**right**) of the left hand of his wife Anna Bertha Ludwig (*Public domain images from Wikimedia Commons.*)

That heavy radiation may induce skin cancer was recognised already in 1902⁽⁸²⁾. In 1928 the International Commission on Radiological Protection (ICRP) was established by the International Congress of Radiology. The three fundamental principles of radiological protection stated by the commission are: justification, optimisation and application of dose limits⁽⁵⁾. The early recommendations concentrated on avoiding threshold effects of radiation. By 1954 the support for the linear-non-threshold model increased, as excess mortality from leukaemia was seen among radiologists in the 1940's and 1950's⁽⁸³⁻⁸⁵⁾. In addition, the long-term follow-up of Japanese survivors of the atomic bomb blasts in Hiroshima and Nagasaki August 1945 had provided important information on radiation induced cancer risk⁽⁸⁶⁾. Most of the radiation induced leukaemia deaths occurred during the first 15 years after exposure. For solid cancers the pattern of excess risk was found to be a life-long elevation of the natural age-specific cancer risk. About 20% of excess cancer deaths among atomic bomb survivors were from leukaemia. In 1966 the term ALARA (As Low As Reasonably Achievable) was coined by the ICRP⁽⁵⁾.

The adverse health effects of radiation exposure are often grouped into two general categories:

- Deterministic effects, which appear when the radiation dose to the tissue exceeds a given threshold dose, cause death or malfunction of cells, such as skin injury, loss of hair or cataracts. Above the threshold dose severity of the injury increases with dose⁽⁸⁷⁾.
- Stochastic (random) effects, i.e. cancer and heritable effects. The risk of injuries in a population exposed to ionizing radiation increases with increasing dose, according to the linear-non-threshold model, but not the severity of disease⁽⁸⁷⁾.

Cells that divide rapidly are more susceptible to radiation, thus children are more sensitive to radiation compared with adults^(2, 3). Furthermore, sometimes radiation induced cancer has a long latency period and, as children have a longer presumed length of life than adults, cancer risk for children is higher^(2, 3).

Effective dose

Effective dose calculations are performed to estimate the risk of stochastic effects to an average member of an irradiated population⁽⁸⁷⁾, and to determine the risk for the entire body from exposure of a part of the body. The definition of the effective dose is based on mean doses to organs or tissues in the human body, and takes into account a given exposure situation but not the characteristics of a specific individual⁽⁵⁾. Consequently, effective dose calculations are not intended for estimating the radiation risk to a specific individual. In addition, effective dose calculations are based on

simulated phantom examinations, and do not take into account age or sex, which also should be included when assessing the risk for cancer^(87, 88).

The *absorbed dose* (in Gy, J/kg) is the energy imparted per unit mass by ionizing radiation in an organ or tissue, and can be directly measured. The unit can be used to estimate the severity of deterministic effects after radiation exposure of an organ or part of the body. By multiplying the mean absorbed dose from radiation in a tissue or an organ with the *radiation weighting factor* the *equivalent dose* (in mSv) is obtained. The radiation weighting factor takes into account the biological effects of radiation, and is 1 for X-rays. The sensitivity and risk of radiation-induced cancer differ between different tissues and organs of the body, therefore *tissue weighting factors* have been introduced. The factors have been determined for 14 different organs or tissues. The highest weightings are given the lungs (0.157) and breasts (0.139), and the sum of all weightings is 1⁽⁵⁾. The *effective dose* (in mSv) is the tissue-weighted sum of the equivalent doses in all specified tissues and organs of the body⁽⁵⁾.

The *effective dose* can be calculated by multiplying the *dose-area-product (DAP)* with a specific *conversion factor* (E_{DAP}):

$$E = E_{\text{DAP}} \times \text{DAP}$$

DAP is the product of the irradiated surface area multiplied by the radiation dose at the surface (Gy cm^2). In the current study it was automatically calculated by the X-ray system. The conversion factor (mSv/Gy cm^2) depends on the type of examination, exposure settings and patient size.

PCXMC software for Monte Carlo simulations

In the PCXMC software for Monte Carlo simulations⁽⁸⁹⁾, developed by STUK (Radiation and Nuclear Safety Authority in Finland), organ doses as well as effective doses can be calculated. In the software programme a set of mathematical phantoms⁽⁹⁰⁾ for ages 0, 1, 5, 10 and 15 years and for adults are predefined.

The software program calculates organ doses from monochromatic photons in 10 kV wide energy bins. Simulations for bins up to 150 kV using 10^7 photons were performed in the present study. The mean value of energy deposited is scored for each organ specified. All organs specified in ICRP 60⁽⁹¹⁾ as well as in ICRP 103⁽⁵⁾ are included for the dose calculations. The effective dose is calculated according to the spectra in the software and the cut-off energy used.

Conversion factors

The conversion factor E_{DAP} (mSv/Gy cm²) is given by the following relation:

$$E_{\text{DAP}} = E / \text{DAP}$$

where E is the effective dose (mSv) and DAP is the dose-area-product (Gy cm²). To determine the conversion factors the DAP value in the PCXMC system is set to 1; consequently the conversion factor is equal to the calculated effective dose. In the simulation described in the current study the zero degree projection, i.e. the scout view, was used in accordance with Svalkvist *et al.*⁽⁹²⁾ to be representative of the entire chest tomosynthesis examination, i.e. scout and tomosynthesis acquisition.

Aims

Paper I

- To illustrate chest imaging findings of cystic fibrosis using tomosynthesis, in comparison with radiography and computed tomography

Paper II

- To design and validate a scoring system for tomosynthesis in pulmonary cystic fibrosis

Paper III

- To analyse and compare the plethora of radiographic scoring systems for cystic fibrosis, with special reference to which scoring components are considered most important

Paper IV

- To determine conversion factors for chest tomosynthesis in children for estimation of the effective dose from the dose-area-product

Paper V

- To determine the paediatric effective dose for chest tomosynthesis

Methods

Paper I–III

A prospective study on cystic fibrosis patients started in 2008, approved by the local ethics committee (DNR 2008/268, 2008/670, 2010/306). When patients were examined with chest radiography or CT for clinical reasons, the examination was supplemented with tomosynthesis after informed consent.

Imaging findings of pulmonary cystic fibrosis

Tomosynthesis is a new method for evaluating cystic fibrosis changes of the lungs. The purpose of the first study was to investigate how different stages of pulmonary cystic fibrosis are depicted with tomosynthesis, compared with radiography and computed tomography. At the time of the Pictorial Review the study population included 36 children (8 to 18 years) with a total of 92 tomosynthesis examinations, and 39 adults (19 to 59 years) with a total of 43 tomosynthesis examinations. In 125 cases the reason for the examination was a yearly check-up and 10 patients were examined due to an exacerbation of the disease. During the study period 12 CT examinations of the chest were performed in nine of the patients for clinical reasons.

The tomosynthesis, radiography and CT examinations were evaluated and compared. From the clinical files a number of cases were selected to illustrate and describe the typical imaging findings of cystic fibrosis, for different stages of the disease. The imaging modalities were also compared regarding cost and radiation dose.

Development of the tomosynthesis scoring system

After a thorough survey of the literature on cystic fibrosis scoring systems for radiography and CT, none of the previously described scoring systems was considered suitable for the scoring of tomosynthesis examinations. Therefore, a scoring system dedicated to tomosynthesis in pulmonary cystic fibrosis was designed. The scoring system was developed in consensus by three paediatric radiologists and one chest radiologist. Before the scoring commenced several learning sessions were held where

the radiologists together scored examinations not included in the study, to ensure that all radiologists were familiar with the scoring system.

In the scoring system the lungs were scored for severity and extent of five well-recognized pathological changes in cystic fibrosis: overinflation, bronchial wall thickening, parenchymal lesions, bronchiectasis and mucus plugging. A scoring form was created with clear definitions of the scoring components and scoring levels (Fig. 4), and reference images were selected from examinations not included in the study.

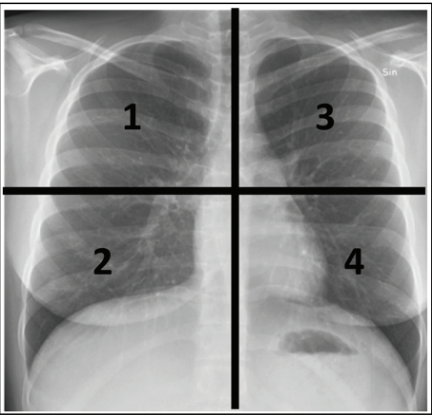
Validation of the scoring system

Examinations used in the development of the scoring system, and in the reference image file, were excluded from the validation. Thus, at the time of the validation of the scoring system the cystic fibrosis study population included 31 children and teenagers (13 M, 18 F, mean age 13, range 8–19 years) and 31 adults (17 M, 14 F, mean age 30, range 20–59 years). Seven children or teenagers without cystic fibrosis (6 M, 1 F, mean age 13, range 8–19 years), screened for lung metastases with normal imaging findings, examined as part of a different study, were also included to provide normal baseline studies. Four paediatric cystic fibrosis tomosynthesis examinations were excluded due to motion artefacts. Thus, 88 pairs of chest radiographs and tomosynthesis examinations from 67 patients remained.

Two paediatric radiologists and one chest radiologist independently scored the anonymised examinations. First the chest radiograph was scored using the Brasfield scoring system⁽⁵¹⁾, and then the corresponding chest tomosynthesis examination was scored using the new tomosynthesis scoring system (Fig. 4).

Cohen's kappa with quadratic weighting and percentage agreement⁽⁹³⁾ were used for assessment of agreements between observers for total disease severity scores and subscores of the tomosynthesis score. Quantification of the disagreement between paired ordered categorical classifications was done using the method by Svensson and Holm^(94, 95).

THE TOMOSYNTHESIS CYSTIC FIBROSIS SCORING FORM

Patient name			<p>4 lung quadrants:</p> <p><i>The lungs are divided at the level of the first division of the left main bronchus</i></p> <p>1= Right upper 2= Right lower 3= Left upper 4= Left lower</p>
Patient ID			
Study date			
Study ID			
Scorer			
Scoring date			
Total score (max 100)			

1) OVERINFLATION

Both lungs are scored (PA/AP and lateral radiographs)
Overall impression (0-4):

0 ☐ None
1 ☐ Mild
2 ☐ Moderate
3 ☐ Severe
4 ☐ Very severe

Score:
(max 4)

3) PARENCHYMAL LESIONS

Rate each quadrant for atelectasis or consolidation (0-4)

Small consolidation is defined as less than the volume of the 7th thoracic vertebra.

Quadrant 1

0 ☐ None
1 ☐ = b
2 ☐ = c
3 ☐ = d
4 ☐ = e

Quadrant 3

0 ☐ None
1 ☐ = b
2 ☐ = c
3 ☐ = d
4 ☐ = e

Quadrant 2

0 ☐ None
1 ☐ = b
2 ☐ = c
3 ☐ = d
4 ☐ = e

Quadrant 4

0 ☐ None
1 ☐ = b
2 ☐ = c
3 ☐ = d
4 ☐ = e

Sum of scores:
(max. 16)

2) BRONCHIAL WALL THICKENING

*Parallel line densities or end-on circular densities.
Normally bronchi peripheral of the central part of the segmental bronchi are **not** visible on tomosynthesis sections.*

Rate each quadrant for bronchial wall thickening (0-4)

Quadrant 1

0 ☐ None
2 ☐ Present
4 ☐ Marked

Quadrant 3

0 ☐ None
2 ☐ Present
4 ☐ Marked

Quadrant 2

0 ☐ None
2 ☐ Present
4 ☐ Marked

Quadrant 4

0 ☐ None
2 ☐ Present
4 ☐ Marked

Sum of scores:
(max. 16)

Fig. 4a

4) BRONCHIECTASIS

A non-tapering bronchus (cylindrical, varicose or cystic); or broncho-arterial ratio > 1 ; or a visible bronchus close to the pleura.
If a bronchiectatic bronchus divides into two dilated branches, only the branches are counted.

A) Rate each quadrant for the **NUMBER** of bronchiectatic bronchi (0-4)

Quadrant 1 0 <input type="checkbox"/> None 1 <input type="checkbox"/> 1-5 2 <input type="checkbox"/> 6-10 3 <input type="checkbox"/> 11-15 4 <input type="checkbox"/> >15	Quadrant 3 0 <input type="checkbox"/> None 1 <input type="checkbox"/> 1-5 2 <input type="checkbox"/> 6-10 3 <input type="checkbox"/> 11-15 4 <input type="checkbox"/> >15
Quadrant 2 0 <input type="checkbox"/> None 1 <input type="checkbox"/> 1-5 2 <input type="checkbox"/> 6-10 3 <input type="checkbox"/> 11-15 4 <input type="checkbox"/> >15	Quadrant 4 0 <input type="checkbox"/> None 1 <input type="checkbox"/> 1-5 2 <input type="checkbox"/> 6-10 3 <input type="checkbox"/> 11-15 4 <input type="checkbox"/> >15

Sum of scores:
(max. 16)

B) Rate each quadrant for the **APPEARANCE** of the widest bronchiectasis (0-4)

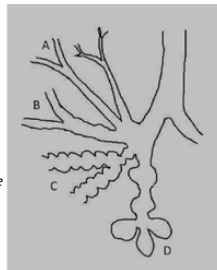
Cylindrical (A, B) = bronchi are mildly and uniformly dilated, with a relatively straight outline.

Subtle cylindrical (A) = discretely dilated, straight outline

Markedly cylindrical (B) = clearly dilated, slightly irregular outline

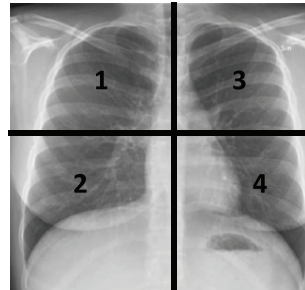
Varicose (C) = bronchi are moderately dilated and local constrictions give the airway an irregular or beaded outline.

Cystic (D) = bronchi are severely dilated giving the airways a ballooned appearance, with strings of cysts or grape-like clusters in the peripheral part of the bronchi.



Quadrant 1 0 <input type="checkbox"/> Not applicable 1 <input type="checkbox"/> Subtle cylindrical 2 <input type="checkbox"/> Markedly cylindrical 3 <input type="checkbox"/> Varicose 4 <input type="checkbox"/> Cystic	Quadrant 3 0 <input type="checkbox"/> Not applicable 1 <input type="checkbox"/> Subtle cylindrical 2 <input type="checkbox"/> Markedly cylindrical 3 <input type="checkbox"/> Varicose 4 <input type="checkbox"/> Cystic
Quadrant 2 0 <input type="checkbox"/> Not applicable 1 <input type="checkbox"/> Subtle cylindrical 2 <input type="checkbox"/> Markedly cylindrical 3 <input type="checkbox"/> Varicose 4 <input type="checkbox"/> Cystic	Quadrant 4 0 <input type="checkbox"/> Not applicable 1 <input type="checkbox"/> Subtle cylindrical 2 <input type="checkbox"/> Markedly cylindrical 3 <input type="checkbox"/> Varicose 4 <input type="checkbox"/> Cystic

Sum of scores:
(max. 16)



4 lung quadrants:
1= Right upper
2= Right lower
3= Left upper
4= Left lower

5) MUCUS PLUGGING

A) Rate each quadrant for **LARGE** mucus plugs (0-4)

Large mucus plugs are tubular opacities with or without a branching pattern or rounded opacities, $\geq 5\text{mm}$, differentiated from vessels by their continuity with bronchi.

Quadrant 1 0 <input type="checkbox"/> None 1 <input type="checkbox"/> In 1-2 bronchi 2 <input type="checkbox"/> In 3-4 bronchi 3 <input type="checkbox"/> In 5-6 bronchi 4 <input type="checkbox"/> In ≥ 7 bronchi	Quadrant 3 1 <input type="checkbox"/> None 2 <input type="checkbox"/> In 1-2 bronchi 3 <input type="checkbox"/> In 3-4 bronchi 4 <input type="checkbox"/> In 5-6 bronchi 5 <input type="checkbox"/> In ≥ 7 bronchi
Quadrant 2 0 <input type="checkbox"/> None 1 <input type="checkbox"/> In 1-2 bronchi 3 <input type="checkbox"/> In 3-4 bronchi 4 <input type="checkbox"/> In 5-6 bronchi 5 <input type="checkbox"/> In ≥ 7 bronchi	Quadrant 4 0 <input type="checkbox"/> None 1 <input type="checkbox"/> In 1-2 bronchi 2 <input type="checkbox"/> In 3-4 bronchi 3 <input type="checkbox"/> In 5-6 bronchi 4 <input type="checkbox"/> In ≥ 7 bronchi

Sum of scores:
(max. 16)

B) Rate each quadrant for **SMALL** mucus plugs (0-4)

Small mucus plugs are seen as clustered small nodular opacities ($< 5\text{mm}$) or as a tree-in-bud pattern in the periphery of the lobes. A **minor area** is defined as less than the volume of the 7th thoracic vertebra.

Quadrant 1 0 <input type="checkbox"/> none 1 <input type="checkbox"/> = b 2 <input type="checkbox"/> = c 3 <input type="checkbox"/> = d 4 <input type="checkbox"/> = e	b) Clustered small mucus plugs in 1-2 minor areas* c) Clustered small mucus plugs in 3-4 minor areas* d) Clustered small mucus plugs in 5-6 minor areas* e) Clustered small mucus plugs in ≥ 7 minor areas* * or a larger area of equivalent size	Quadrant 3 0 <input type="checkbox"/> none 1 <input type="checkbox"/> = b 2 <input type="checkbox"/> = c 3 <input type="checkbox"/> = d 4 <input type="checkbox"/> = e
Quadrant 2 0 <input type="checkbox"/> none 1 <input type="checkbox"/> = b 2 <input type="checkbox"/> = c 3 <input type="checkbox"/> = d 4 <input type="checkbox"/> = e		Quadrant 4 0 <input type="checkbox"/> none 1 <input type="checkbox"/> = b 2 <input type="checkbox"/> = c 3 <input type="checkbox"/> = d 4 <input type="checkbox"/> = e

Sum of scores:
(max. 16)

Fig. 4b

The scoring form of the tomosynthesis scoring system. (Fig. 2 in Paper II, reproduced with permission.)

Comparison of scoring systems for cystic fibrosis

Selection of scoring systems

From a survey of the literature and a search in PubMed, followed by a manual perusal of references in the selected articles to locate all published scoring systems, a total of 28 scoring systems was found: 12 for radiography⁽⁴⁷⁻⁵⁸⁾, one for tomosynthesis⁽⁴²⁾, 14 for CT⁽⁶³⁻⁷⁶⁾, and one for MRI⁽⁴⁶⁾. To select the most widely used scoring systems for the current review, scoring systems for radiography and CT with 25 or more citations in the Citation Index of the Web of Science database⁽⁹⁶⁾ were selected for analysis. The scoring systems for tomosynthesis and MRI were published in 2012; consequently both systems yet had fewer citations in the Web of Science database.

Seven cystic fibrosis scoring systems for chest radiography with 25 or more citations were found in the Web of Science database, but three systems⁽⁴⁷⁻⁴⁹⁾ were excluded since the scores are part of clinical scores and other authors have shown that the Brasfield score⁽⁵¹⁾ is superior to those scoring systems^(97, 98). Thus four radiography scoring systems remained for analysis: The Chrispin-Norman scoring system from 1974⁽⁵⁰⁾, the Brasfield scoring system from 1979⁽⁵¹⁾, the Wisconsin scoring system from 1993⁽⁵⁵⁾, and the Northern scoring system from 1994⁽⁵⁶⁾.

Nine chest CT cystic fibrosis scoring systems with 25 or more citations were found in the Web of Science database, but the Brody I scoring system⁽⁷⁰⁾ was excluded from the comparison due to the development of the Brody II scoring system⁽⁷⁵⁾. Thus eight CT scoring systems remained for analysis: Bhalla⁽⁶⁴⁾ and Nathanson⁽⁶³⁾ from 1991, Maffessanti from 1996⁽⁶⁶⁾, Shah from 1997⁽⁶⁸⁾, Santamaria from 1998⁽⁶⁹⁾, Helbich from 1999⁽⁷¹⁾, Robinson from 2001⁽⁷³⁾, and Brody II from 2004⁽⁷⁵⁾. The scoring systems by Shah⁽⁶⁸⁾, Santamaria⁽⁶⁹⁾, Helbich⁽⁷¹⁾, and Robinson⁽⁷³⁾ are developed from the Bhalla scoring system⁽⁶⁴⁾.

Analysis of scoring systems

The analysis of the scoring systems included an evaluation of:

1. The abnormalities scored (i.e. the scoring components)
2. The area scored for the components in each system
3. The number of scoring levels used for each component
4. The calculations needed to reach the final score
5. The weighting applied to each component as a percentage of the total score

Paper IV–V

To determine the effective dose from chest tomosynthesis the DAP value, which was automatically registered by the X-ray system used in the current study, is multiplied by a conversion factor. For chest tomosynthesis in adults the conversion factor of 0.26 mSv/Gycm²⁽⁹⁹⁾ has been reported, and the effective dose has been determined to 0.12–0.13 mSv^(99, 100). The purpose of study IV was to determine conversion factors for paediatric chest tomosynthesis by Monte Carlo simulations (See Background). These conversion factors were used in study V to estimate the effective dose from registered DAP values from patient examinations.

Conversion factor determination

The built-in phantoms in the PCXMC software were modified using data on the average weight and height of Swedish boys and girls⁽¹⁰¹⁾ for ages 8 to 19 years. Simulations for children younger than 8 years were not performed, as they in general have compliance difficulties with holding their breath for the approximately 10 seconds required for the tomosynthesis sweep.

The irradiated area in the PCXMC graphics window was set to be the same for all used age and sex specific combinations. The anode angle was set to 12.5 degrees. The focus-to-detector distance for posteroanterior (PA) was 180 cm, for anteroposterior (AP) exposures 100 cm. The focus-to-detector distance included an air gap of 5 cm, which is the setting in the tomosynthesis system used at our department (Definium 8000 with VolumeRAD option; GE Healthcare, Chalfont St Giles, UK).

Conversion factors for chest tomosynthesis were determined for both sexes for ages 8–19 years for the PA projection and for ages 8–12 years for the AP projection, with tube voltage settings between 80 and 140 kV. An inherent filtration with 2.7 mm Al was used together with 0.2 mm Cu additional filtration. To determine the effect of increased copper filtration on the conversion factor, simulations were also performed with 0.1, 0.2 and 0.3 mm Cu filtration with the tube energy of 120 kV for the PA projection and 107 kV for the AP projection. These are the settings currently recommended by the manufacturer for all patients, independent of age.

In order to validate the results a comparison was made with the results by Svalkvist *et al.*⁽⁹²⁾, by simulations on an adult phantom (170 cm/ 70 kg, 120 kV), using the same filtrations as used in the previous study (3 mm Al and 0.1 mm Cu), as well as the filtrations used in the current study (2.7 mm Al and 0.2 mm Cu). To evaluate the effect of collimation on the conversion factors simulations were performed with four different collimations, standard and 0.5 cm, 1.0 cm and 1.5 cm increase in height and width of the aperture size, respectively.

Effective dose determination in a paediatric patient population

During a three-year-period 186 chest tomosynthesis examinations were performed on 74 patients (40 M and 34 F), mean age at the time of the examinations 13.7 years, range 7–20 years. The patients, 38 children with cystic fibrosis and 36 paediatric oncology patients screened for lung metastases, were examined as part of two different prospective studies, approved by the local ethics committee and with informed written consent from all patients or legal guardians. In all cases height and weight of the patients close in time to the tomosynthesis examination were recorded. Out of 63 examinations performed on children 12 years or younger, 17 examinations were performed AP. The remaining 169 examinations were performed PA.

For all examinations separate DAP values, tube voltage settings (kV) and tube load settings (mAs) were available for the full examination (i.e. scout view + tomosynthesis acquisition + lateral projection), as well as for the tomosynthesis scout and for the lateral projection (which was performed for diagnostic purposes). The DAP value was calculated by the X-ray system from the selected collimation, energy, tube load and copper filtration. By subtracting the DAP values of the scout and lateral projections from the DAP value of the full examination the DAP value for the tomosynthesis acquisition was calculated.

The effective dose (E, mSv) could be calculated from the registered DAP values by using the same formula as used in the Monte Carlo simulations (described in more detail the Background chapter):

$$E = E_{\text{DAP}} \times \text{DAP}$$

where DAP (Gy cm^2) is the dose-area-product as calculated by the X-ray equipment during the exposure and E_{DAP} is the conversion factor in mSv/Gy cm^2 .

The corresponding sex, age and energy corrected conversion factor reported in Paper IV⁽¹⁰²⁾, based on ICRP 103 organ weighting⁽⁵⁾, was selected for each examination to calculate the effective dose from the DAP values. In addition the effective dose was calculated using the simplified age-dependent conversion factors for PA exposure of 0.6 (8–10 years), 0.4 (11–14 years) and 0.3 mSv/Gy cm^2 (15–19 years) proposed in Paper IV; the conversion factor proposed by B  th *et al.*⁽⁹⁹⁾ for tomosynthesis of 0.26 mSv/Gy cm^2 and the well-established conversion factor for chest radiography of 0.18 mSv/Gy cm^2 ⁽¹⁰³⁾.

Phantom examinations

In view of the considerable variations in the registered DAP values for paediatric chest tomosynthesis examinations at our institution, which could not fully be explained by

patient variability regarding body size or age, phantom examinations were performed. The aim was to explain the reason for this unexpected variability.

The aim of the *first part* of the phantom examinations was to investigate if instabilities of the X-ray system and the detector, i.e. variations in output, could influence the registered DAP values. An experienced technician performed 16 tomosynthesis examinations on an adult Sectional Chest Phantom, SK200 (The Phantom Laboratory, NY, USA) at two separate days, with the same kV and mA settings.

The aim of the *second part* of the phantom examinations was to investigate if differences in how the technicians performed the examinations, e.g. by using different exposure settings, collimation or patient positioning, could explain the variability in registered DAP values for the patient examinations. The adult chest phantom and a paediatric chest phantom (Pedo-RT-humanoid phantom, Humanoid systems, Carson, USA), corresponding to age 6 years, were repeatedly examined with tomosynthesis by seven technicians, with a total of 33 examinations per phantom.

Results

Paper I

Pulmonary changes in cystic fibrosis are more clearly depicted with tomosynthesis compared with radiography, and most changes seen with CT can also be visualised well with tomosynthesis.

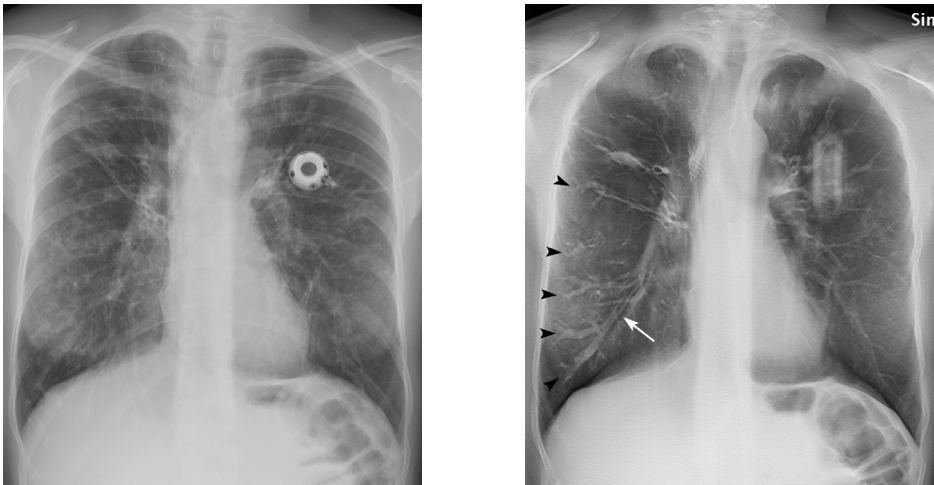


Fig. 5
47-year-old woman with cystic fibrosis. The posteroanterior radiograph (**left**) shows moderate cystic fibrosis changes and suspected mucus plugs in the right lung. On a tomosynthesis section (**right**) the mucus plugs (*arrowheads*) and cylindrical bronchiectasis (*white arrow*) are depicted more clearly. Out-of-plane artefacts from a central venous access device are seen in the left upper quadrant. (*Author's image.*)

In the normal healthy lung the *bronchial walls* are visible in the central lung with tomosynthesis, but not in the periphery. When bronchi are thickened they are clearly delineated with tomosynthesis, not only centrally, but also in the periphery. Small *mucus plugs* are usually not visible on radiographs but can be seen with tomosynthesis as tree-in-bud patterns or as small clustered nodules in the periphery of the lobes (Figs. 5 and 6). The appearance is similar on coronal CT scans (Figs. 7 and 8). Large

mucus plugs can be seen as blurred nodular or cylindrical shadows on radiographs, but are with tomosynthesis sharply depicted inside the bronchi (Figs. 5 and 7).

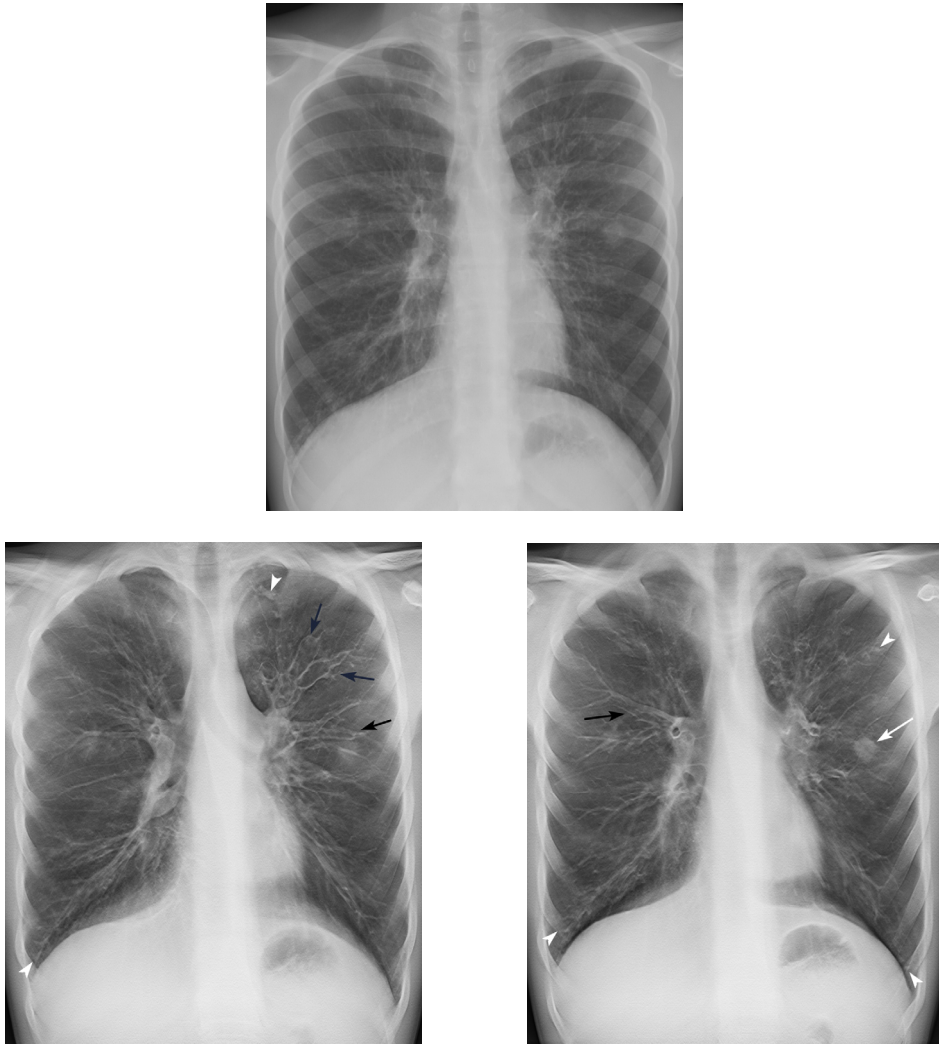


Fig. 6
15-year-old boy with cystic fibrosis. The PA radiograph (**top**) shows mild to moderate general changes of cystic fibrosis; with increased linear markings and a nodular opacity lateral of the left hilum. Bronchiectasis is suspected in the upper parts of both hilar regions. A tomosynthesis section (**bottom left**) shows the cystic fibrosis changes in more detail, with general bronchial wall thickening, varicose bronchiectasis (*black arrows*) and small mucus plugs (*arrowheads*) clearly depicted as tree-in-bud patterns on the right side. Another tomosynthesis section (**bottom right**) shows the small parenchymal consolidation more clearly (*white arrow*), as well as bronchiectasis (*black arrow*) and mucus plugs (*arrowheads*). (Author's image.)

Bronchiectasis may be clearly visualized with CT, but are often difficult to assess with radiography. Radiographs depict suspicious bronchiectasis as increased linear markings or blurred cystic lesions; with tomosynthesis it is possible to differentiate them in detail as cylindrical, varicose, or cystic bronchiectasis (Fig. 5 and 6). When the examination is performed upright air-fluid levels might be observed in the bronchiectasis or in abscesses, and small air-fluid levels seen on tomosynthesis are especially easy to miss on radiography.

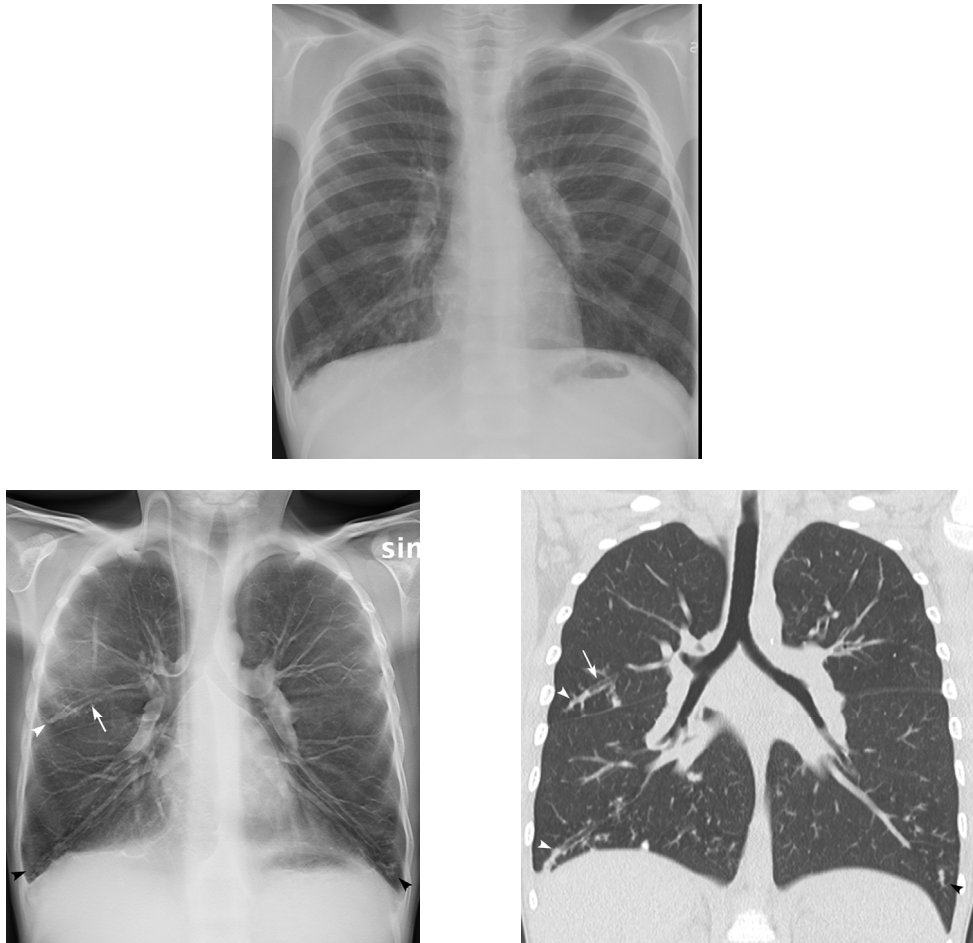


Fig. 7
8-year-old boy with cystic fibrosis. The PA radiograph (**top**) shows mild cystic fibrosis changes, with suspected mucus plugs in the right lower lobe. On tomosynthesis (**bottom left**) and CT (**bottom right**) sections mucus plugs (*arrowheads*) and bronchiectasis (*arrows*) are clearly visualised. (*Author's image.*)

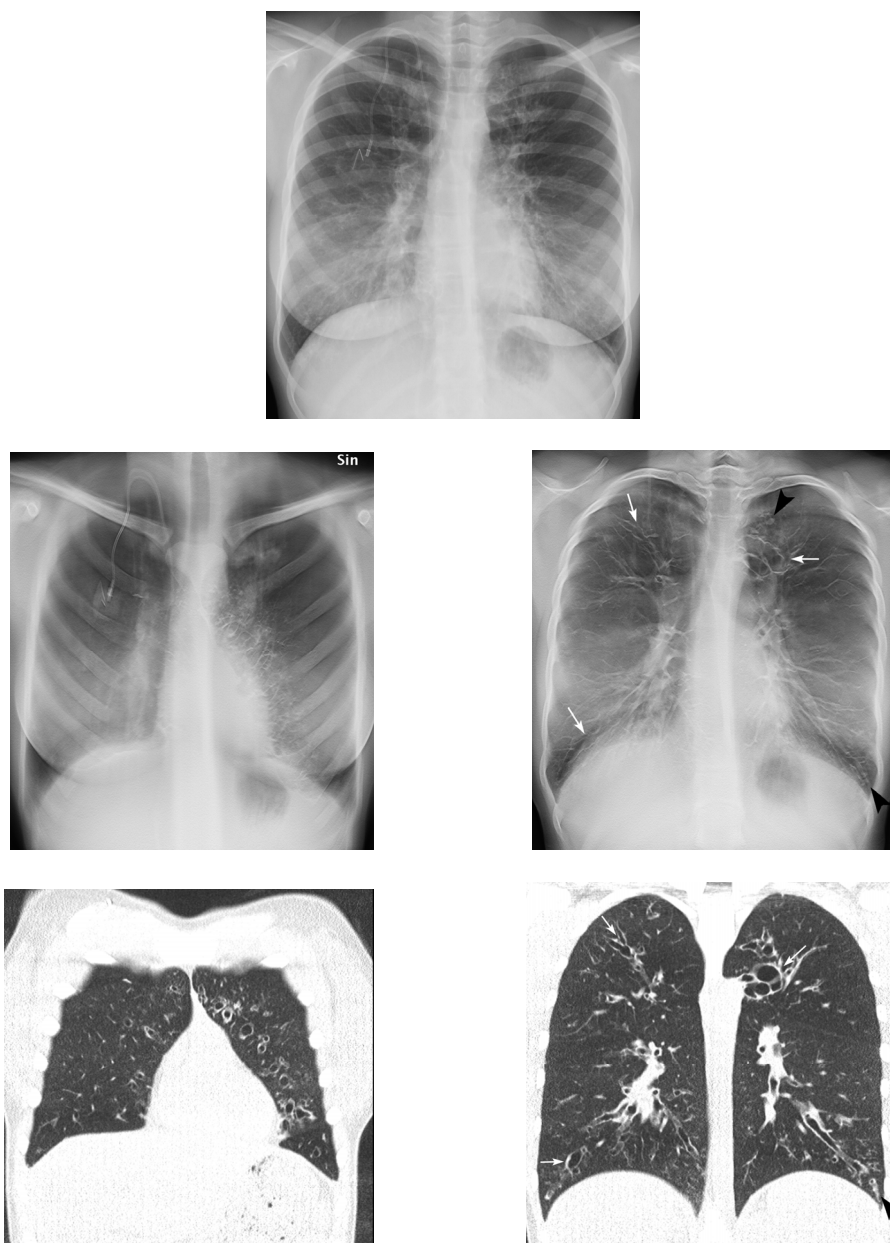


Fig. 8
 15-year old girl with cystic fibrosis. The PA radiograph (**top**) shows suspicious bronchiectasis in perihilar regions. The tomosynthesis (**middle**) and CT sections (**bottom**) show almost identical findings, with bronchiectasis along the left anterior heart border, and in both upper and lower lobes (*arrows*) and small areas of mucus plugging in the left lower lobe (*arrowheads*). (*Author's image.*)

Localized *air trapping* and *mosaic pattern*, which often are well assessable with CT, cannot be adequately evaluated with tomosynthesis. These findings can be suspected with tomosynthesis if there is an absence of vascular markings or an area of hyperlucent lung. *Bullae* are more clearly delineated with tomosynthesis than with radiography, but can be seen in more detail with CT.

As tomosynthesis depicts the lungs in the coronal plane with contiguous slices it gives a better overview of the bronchial tree compared to traditional axial high resolution CT images with 10 mm interspace. In our opinion sequential studies are easier to compare when the whole volume of the lungs is included in tomosynthesis examinations or in volume CT of the lungs, which now has replaced traditional axial high resolution CT at many centres.

Paper II

The tomosynthesis scoring system is presented in Fig. 4 and in more detail in the original publication⁽⁴²⁾ (see Appendix). The Electronic supplementary material is available at the publisher's website⁽⁴²⁾. The scoring system proved to be robust, when comparing the results of the scoring performed by three independent observers. Interobserver agreements for the total disease severity score in the tomosynthesis scoring showed almost perfect correlation with kappa values >0.90 for the three pairs of observers (Fig. 9). The observer agreements for all subscores were also high.

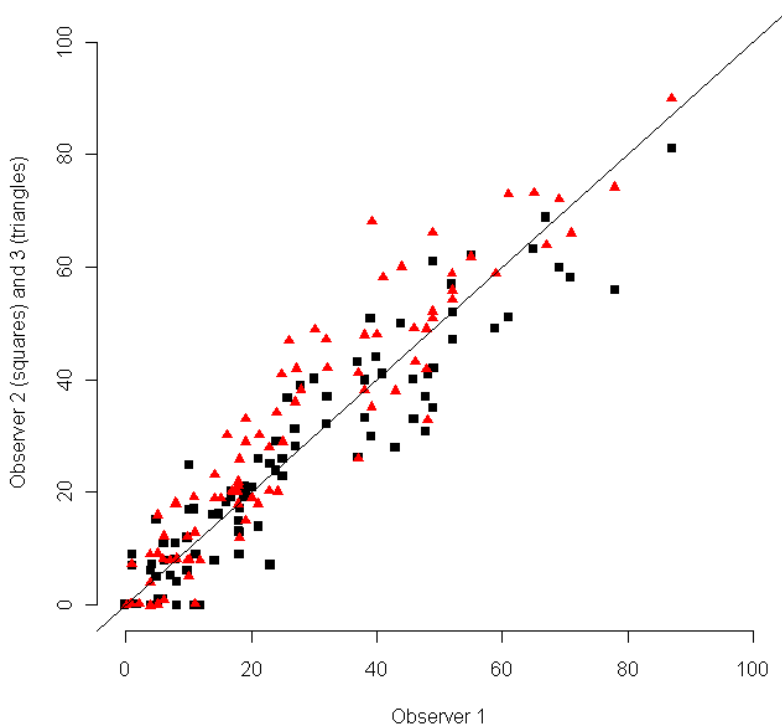


Fig. 9

Comparison of total disease severity scores for tomosynthesis between observers (*black squares* observer 1 vs. observer 2; *red triangles* observer 1 vs. observer 3). (Fig. 4 in Paper II⁽⁴²⁾, reproduced with permission.)

Observer agreements for total disease severity scores were almost perfect for scoring of chest radiography using the Brasfield scoring system⁽⁵¹⁾, with kappa values 0.80, 0.81 and 0.85 for the three pairs of observers.

The scoring results for tomosynthesis and for radiography showed good correlation between the total disease severity scores, and Kendall's rank correlation tau was 0.68, 0.77 and 0.78 for the three observers (Fig. 10). Tomosynthesis was generally scored higher with regard to percentage of maximum score, with mean tomosynthesis score for the three observers being 30% of the maximum score and mean Brasfield score of being 24% of the maximum score (Fig. 10 and Table 1).

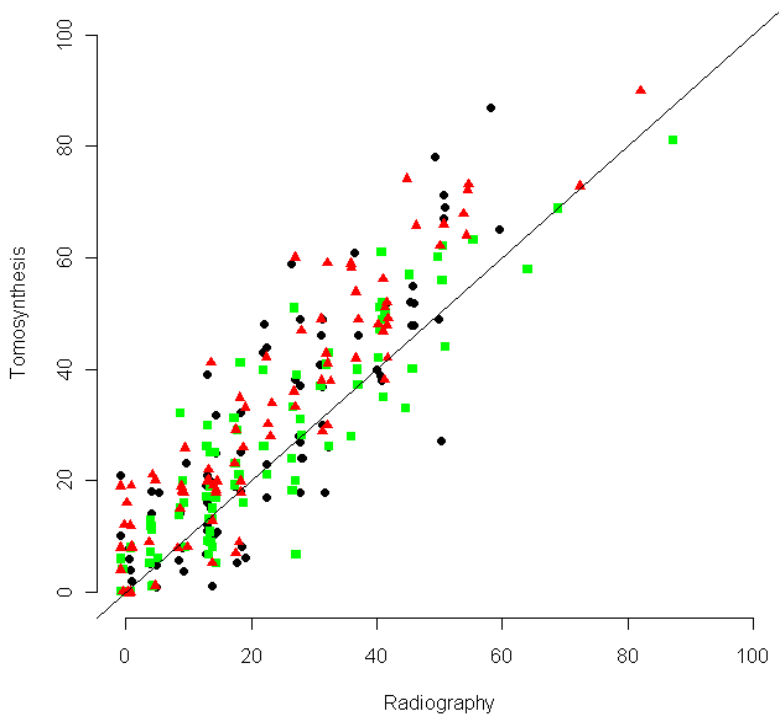


Fig. 10

Comparison of total disease severity scores for radiography and tomosynthesis as a percentage of the maximum score for the three observers (*black dots* observer 1, *green squares* observer 2, *red triangles* observer 3). (Fig. 6 in Paper II ⁽⁴²⁾, reproduced with permission.)

Table 1.

A comparison of the mean total scores for the 88 radiography and tomosynthesis examinations, in percentage of the maximum score. Tomosynthesis was generally scored higher than radiography.

	Radiography		Tomosynthesis	
	No of examinations	In % of all examinations	No of examinations	In % of all examinations
Total mean score				
≤ 25	54	61	48	55
>25 to ≤50	29	33	25	28
>50 to ≤75	4	5	14	16
>75 to 100	1	1	1	1
Min	0		0	
Max	76		86	

Diversity in the tomosynthesis scores was greater than for the Brasfield score. Many patients scored normal for linear markings with radiography, were scored for presence of bronchial wall thickening with tomosynthesis. Patients without apparent nodular cystic lesions on radiographs had bronchiectasis or mucus plugs detectable with tomosynthesis (Fig. 11).

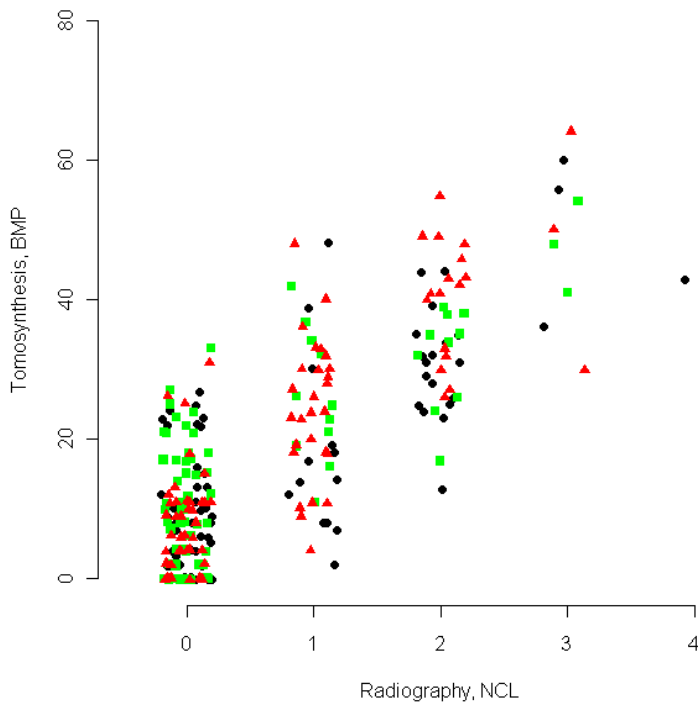


Fig. 11

Comparison of the scores for nodular cystic lesions (NCL) on radiographs with the sum of the scores for bronchiectasis and mucus plugging (BMP) on tomosynthesis sections for the three observers (*black dots* observer 1, *green squares* observer 2, *red triangles* observer 3). (*Fig. 8 in Paper II* ⁽⁴²⁾, reproduced with permission.)

Paper III

Pulmonary abnormalities associated with cystic fibrosis have different appearances depending on the modality chosen to evaluate them. Certain abnormalities can only be evaluated with CT or MRI, as CT has a higher contrast resolution than radiography and tomosynthesis, and MRI is performed with intravenous contrast, enabling detection of perfusion defects (Table 2).

Details on how the scoring is performed in the different scoring systems, with regard to *the abnormalities scored* i.e. the scoring components, *the area scored* for the components in each system, the *number of scoring levels* used for each component, *the calculations needed to reach the final score*, and *the weighting* applied to each component as a percentage of the total score are given in the original publication (Paper III ⁽¹⁰⁴⁾).

Abnormalities scored and scoring areas

Radiography

Radiographic scoring systems use two different scoring approaches. The Northern scoring system⁽⁵⁶⁾ is based on integrated scores for lung areas, while the other three systems^(50, 51, 55) are based on separate scoring components. In the modified Chrispin-Norman scoring system from 2005⁽⁵⁸⁾ as well as in the Northern scoring system⁽⁵⁶⁾ only the frontal radiograph is needed for scoring.

In all reviewed scoring systems for radiography increased lung volume is scored separately, except in the Northern score where it is included in the overall impression score. Bronchial wall thickening, parenchyma, bronchiectasis and mucus plugging are evaluated in all scoring systems, but the nomenclature differs. For example, bronchiectasis and mucus plugging are described as ring shadows and mottled shadows, as bronchiectasis and nodular-branching opacities, or scored together as nodular-cystic lesions. In the Northern⁽⁵⁶⁾ and the Brasfield⁽⁵¹⁾ scoring systems the overall or general severity is also scored.

Tomosynthesis

When the study was carried out only one scoring system for tomosynthesis had been published, see Paper II⁽⁴²⁾.

Both lungs are scored for degree of overinflation on the frontal and lateral radiographs, in comparison with reference images available on the publisher's web site. Each lung quadrant is scored for bronchial wall thickening, parenchymal lesions (e.g. atelectasis or consolidation), number and appearance of bronchiectatic bronchi,

and large (>5 mm) or small (<5 mm) mucus plugs, using all tomosynthesis sections covering the quadrant in question.

Table 2.

A comparison of the four different radiologic modalities regarding the ability to depict cystic fibrosis changes of the lungs (yes or no). If the abnormality only can be depicted when it is very severe or widespread the yes is in parenthesis. (*Adapted from Table 1 in Paper III⁽¹⁰⁴⁾.*)

Evaluated abnormalities		Radiography	Tomosynthesis	CT	MRI
Lung volume	Increased lung volume	Yes	Yes	Yes	No
	Emphysema	No	No	Yes	No
	Air trapping	No	No	Yes	No
Bronchial wall thickening		(Yes) ^a	Yes	Yes	Yes ^b
Bronchiectasis		(Yes) ^a	Yes	Yes	Yes ^b
Mucus plugging		(Yes) ^a	Yes	Yes	Yes
Parenchyma	Consolidation	Yes	Yes	Yes	Yes
	Atelectasis	Yes	Yes	Yes	Yes
	Cysts/bullae	(Yes) ^a	Yes	Yes	(Yes) ^a
	Abscesses	(Yes) ^a	Yes	Yes	Yes
	Thickened septa	No	No	Yes	No
	Mosaic perfusion	No	No	Yes	No
	Ground glass opacities	No	No	Yes	No
Pulmonary perfusion		No	No	No	Yes
Pleural affection		Yes	Yes	Yes	Yes

^a using tomosynthesis or CT these changes are better seen than with radiography and MRI.

^b MRI cannot differentiate between bronchial wall thickening and bronchiectasis, especially in the lung periphery⁽⁴⁶⁾.

Computed tomography

Combined radiographic pathology such as nodular-cystic lesions⁽⁵¹⁾ are resolved into more detail on chest CT and scored separately as mucus plugging and bronchiectasis in the CT scoring systems. Bronchial wall thickening is also seen more clearly on CT. Increased lung volume is scored as emphysema or overinflation. Three of the CT scoring systems score air trapping on expiratory images^(69, 73, 75). The Nathanson CT scoring system⁽⁶³⁾ scores only bronchiectasis and mucus plugging. The other chest CT scoring systems all evaluate bronchial wall thickening, bronchiectasis, mucus plugging, and parenchymal lesions. The Maffessanti system⁽⁶⁶⁾ is an exception, where mucus plugging is regarded as a transient phenomenon and recorded separately from the total score. In addition sacculations and abscesses, air-fluid levels and centrilobular nodules, ground glass opacities, thickening of intra- and inter-lobular septa and mosaic perfusion are scored in some scoring systems.

The chest CT scoring systems score abnormalities per bronchopulmonary segment, 12 zones, six lobes or four regions. In addition, in three scoring systems^(64, 69, 71), for example bronchiectasis is scored both for severity, extent i.e. number of bronchopulmonary segments involved, and for number of generations of bronchial divisions involved. The latter score component also includes mucus plugging.

MRI

As for tomosynthesis, when the study was carried out, only one scoring system had been published for MRI, developed by Eichinger *et al.*⁽⁴⁶⁾.

Six lung lobes, with the lingula considered as a single lobe, are scored for bronchiectasis/wall thickening, mucus plugging, abscess/sacculation, consolidation, special findings and perfusion defect size (after intravenous contrast). Bronchiectasis and bronchial wall thickening are scored as a single entity since the spatial resolution of MRI does not allow for differentiation between them. Special findings relate to pleural affection, reflecting for example pleural effusion, pleural reaction/pleurisy or pneumothorax⁽⁴⁶⁾.

Scoring levels and calculations for the final score

The Chrispin-Norman score⁽⁵⁰⁾ for radiography has three scoring levels (not present, present but not marked, and marked) which are comparable to the Wisconsin scores⁽⁵⁵⁾ (none, mild, and severe) for bronchiectasis and nodular-branching opacities. In the Wisconsin score large opacities are scored as absent or present, and then the numbers of affected lobes are rated. The other scoring systems for chest radiography predominately use five scoring levels.

In the tomosynthesis scoring system⁽⁴²⁾ the scoring components overinflation, parenchymal lesions, bronchiectasis and mucus plugging have five scoring levels (0–4). Bronchial wall thickening has three scoring levels (0–2–4). The most severe score is 4 for all scoring components and subcomponents.

In the scoring systems for CT most components are scored using four levels (0–3). In the Nathanson⁽⁶³⁾ scoring system six levels are used for scoring bronchiectasis, and mucus plugging is scored as absent or present. In the Robinson⁽⁷³⁾ scoring system five levels are used for all components.

In the MRI scoring system⁽⁴⁶⁾ the scoring levels 0–1–2 are used for all parameters, where 1 implies involvement of less than 50% of the lobe and 2 implies involvement of more than 50% of the lobe.

In most scoring systems the final score is calculated by summation of the subscores. But some final scores are derived by complicated mathematics, such as in the Brody II score⁽⁷⁵⁾ for CT, where a theoretical maximum of 243 points cannot be greater than 207, and the resultant score is normalized to a grading from 0 to 100.

Weighting of scoring components

The importance of each scoring component, i.e. the weighting applied to each component as a percentage of the total score, differs between the scoring systems and the modalities used (Fig. 12). In most scoring systems bronchiectasis alone, or in combination with mucus plugging, is given the highest weighting.

In the Chrispin-Norman⁽⁵⁰⁾ and the Wisconsin⁽⁵⁵⁾ scoring systems the combination of bronchiectasis and mucus plugging is given the highest weighting in percentage of the total score. In the Wisconsin score parenchymal changes are also given a high weighting. In the Brasfield score⁽⁵¹⁾ large lesions and general severity are given the highest weightings, while bronchiectasis and mucus plugging are given comparatively low weightings.

In the tomosynthesis scoring system⁽⁴²⁾ the highest weighting is given bronchiectasis and mucus plugging, with 32% each of the maximum score.

In the majority of the CT scoring systems the highest weighting in percentage of the total score is given bronchiectasis. The exceptions are the Robinson⁽⁷³⁾ system where all scoring components are given the same weighting (20%), and the Santamaria⁽⁶⁹⁾ scoring system where parenchymal changes are given the highest weighting (43%).

In the MRI score all components of the score are given the same weighting, 17% of the maximum score. The scores for bronchiectasis together with sacculations/abscesses and mucus plugging contribute to 41 % of the total score.

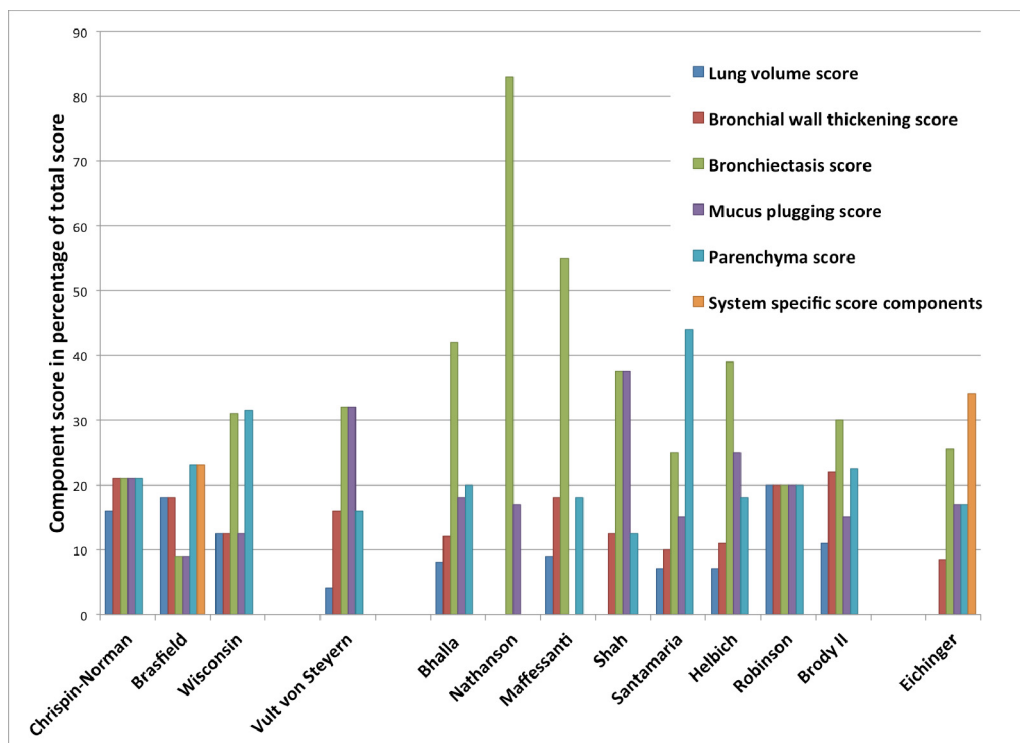


Fig. 12

A comparison of the weighting of scoring components (percentage of total score) in three radiographic scoring systems^(50, 51, 55), one tomosynthesis scoring system⁽⁴²⁾, eight CT scoring systems^(63, 64, 66, 68, 69, 71, 73, 75), and one MRI scoring system⁽⁴⁶⁾. The Brasfield scoring system⁽⁵¹⁾ scores bronchiectasis and mucus plugging together as “nodular cystic lesions”. In the MRI score bronchiectasis and bronchial wall thickening are scored together. In this table these scores are divided between the two entities. “System specific score components” refer to general severity in the Brasfield score and special findings and perfusion size in the MRI score. (*Fig. 2 in Paper III* ⁽¹⁰⁴⁾.)

Paper IV

Conversion factors for paediatric chest tomosynthesis examinations calculated from the phantom simulations ranged between 0.23 and 1.09 mSv/Gycm² depending on age (8–19 years), sex, projection (PA or AP), energy (80–140 kV), Cu filtration (0.1–0.3 mm) and organ weighting (ICRP 60 or ICRP 103).

From 8 to 15 years of age the conversion factor decreased markedly with increasing age, but from age 16 years the conversion factor for the PA projection became fairly independent of age (Fig. 13).

Conversion factors for females below age 14 years were in general slightly lower than for matched males, whereas conversion factors for females above age 14 years were in general slightly higher than for matched males (Fig. 13).

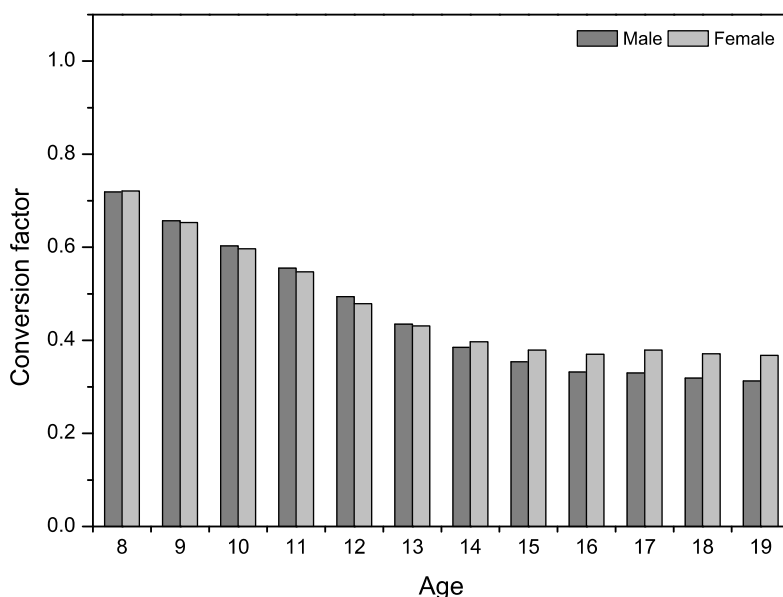


Fig. 13

Conversion factors for PA chest tomosynthesis in children obtained with 120 kV (0.2 mm Cu) based on ICRP 103 organ weighting ⁽⁵⁾. The conversion factor was highest for the youngest children and decreased markedly from 8 to 14 years of age. From the age of 14 years the conversion factor was less age dependent but an increasing difference was seen between the sexes. (Fig. 2 in Paper IV ⁽¹⁰²⁾, reprinted with permission.)

AP projections resulted in 31–46% higher conversion factors than PA projections, with the same tube voltage setting (Fig. 14).

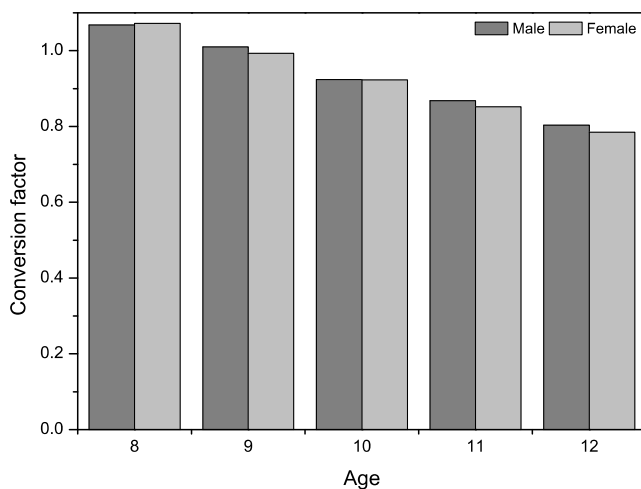


Fig. 14

Conversion factors for AP chest tomosynthesis in children obtained with 107 kV (0.2 mm Cu) based on ICRP 103 organ weighting ⁽⁵⁾. The conversion factors were higher for AP exposures compared with PA exposure, and decreased with age. (*Fig. 3 in Paper IV⁽¹⁰²⁾, reprinted with permission.*)

The ICRP 103⁽⁵⁾ calculated conversion factors for PA exposures were found to be approximately 10% higher (range 6–14%) compared with ICRP 60⁽⁹¹⁾ calculated conversion factors, independent of sex.

With increasing aperture size the conversion factor decreased slightly, but the use of different filtrations had a larger impact on the conversion factors.

The conversion factor increased with increasing tube voltage, more markedly for the PA projection compared with the AP projection. Additional copper filtration increased the conversion factor, but in the AP projection the increase in the conversion factor was less pronounced than in the PA projection (Fig. 15).

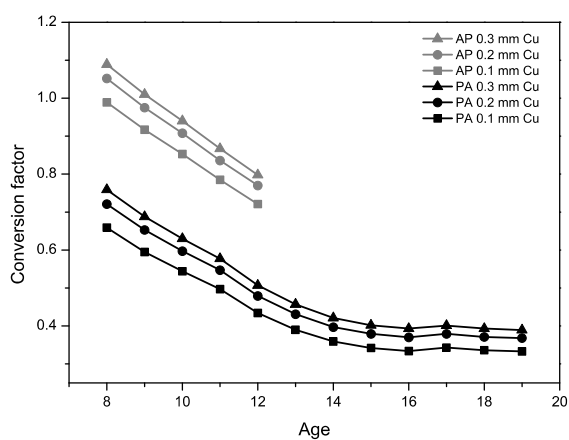
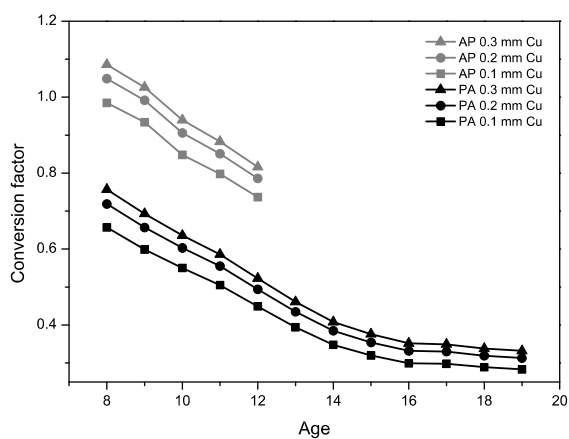


Fig. 15

The effect of copper filtration on the conversion factor for AP (107 kV) and PA (120 kV) chest tomosynthesis for males (top) and females (bottom) of different age (ICRP 103). (Fig. 4 in Paper IV⁽¹⁰²⁾, reprinted with permission.)

Paper V

Effective dose determination in a paediatric patient population

The height and weight of the study population at the time of the chest tomosynthesis examinations were similar to the normal Swedish paediatric population described by Werner and Bodin in 2006⁽¹⁰¹⁾ (Fig. 16).

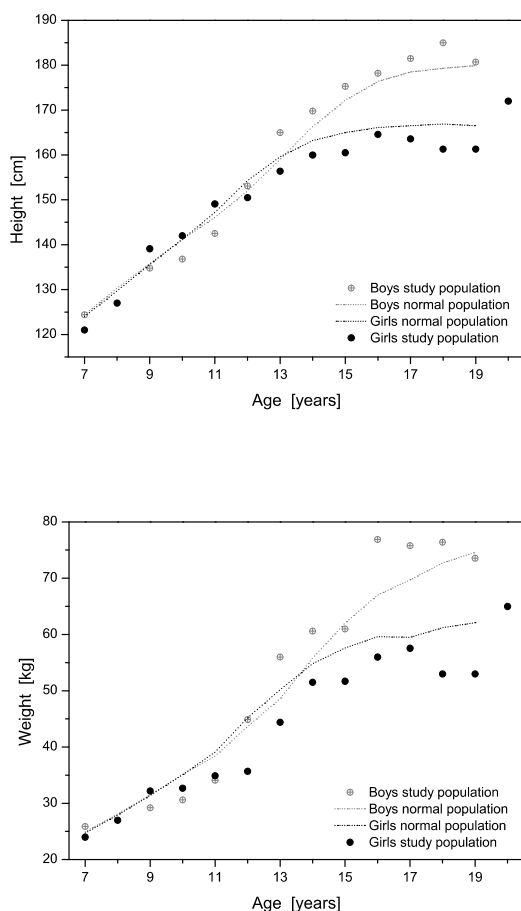


Fig. 16

Mean height (**top**) and weight (**bottom**) of the children in the study at the time of the chest tomosynthesis examinations, was similar to the normal distribution in Swedish children. *Adapted with permission from Werner and Bodin 2006⁽¹⁰¹⁾. (Fig. 1 in Paper V⁽¹⁰⁵⁾, reprinted with permission.)*

Large variations in registered DAP values for patient examinations were seen. DAP values increased with increasing age ($p < 0.0001$), height ($p < 0.0001$), weight ($p < 0.0001$) and BMI ($p < 0.0001$), but did not correlate with sex ($p = 0.36$).

Consequently, the effective dose calculated using the non-corrected conversion factors of 0.26 mSv/Gycm^2 ⁽⁹⁹⁾ and 0.18 mSv/Gycm^2 ⁽¹⁰³⁾ increased markedly with age. The mean effective dose for the PA tomosynthesis examination was 0.11 mSv using the conversion factor 0.26 mSv/Gycm^2 and 0.08 mSv using the conversion factor 0.18 mSv/Gycm^2 .

Using conversion factors corrected for sex, age and energy determined in Paper IV ⁽¹⁰²⁾ the mean effective dose for the PA tomosynthesis examination was 0.17 mSv . The increase in effective dose with age was reduced, but still statistically significant. Using these conversion factors resulted in a wider range of effective doses for the patient population, than if the same conversion factor was used for all examinations.

The mean effective dose calculated for the 169 PA chest tomosynthesis examinations was 0.15 mSv using the simplified conversion factors for PA exposure of 0.6 (8–10 years), 0.4 (11–14 years) and 0.3 mSvGycm^2 (15–19 years) proposed in paper IV ⁽¹⁰²⁾. The scout acquisition contributed approximately to 8% of the DAP value for PA exposure and 6% for AP exposure.

Only 17 of the examinations (13 on boys and 4 on girls) were performed AP. The DAP values were considerably higher than for the PA examinations and consequently also the estimated effective dose, in particular when using the conversion factors corrected for sex, age and energy ⁽¹⁰²⁾. Mean effective dose for the tomosynthesis examination was 0.58 mSv using corrected conversion factors, 0.17 mSv using the conversion factor 0.26 mSv/Gycm^2 ⁽⁹⁹⁾ and 0.12 mSv using the conversion factor 0.18 mSv/Gycm^2 ⁽¹⁰³⁾.

During the study period it was recommended in the local imaging protocol to use the peak energy of 110 kV for patients 7 to 16 years of age, and 120 kV over 16 years of age. The tube voltage was set higher than recommended in 125 of 169 PA tomosynthesis examinations (Fig. 17).

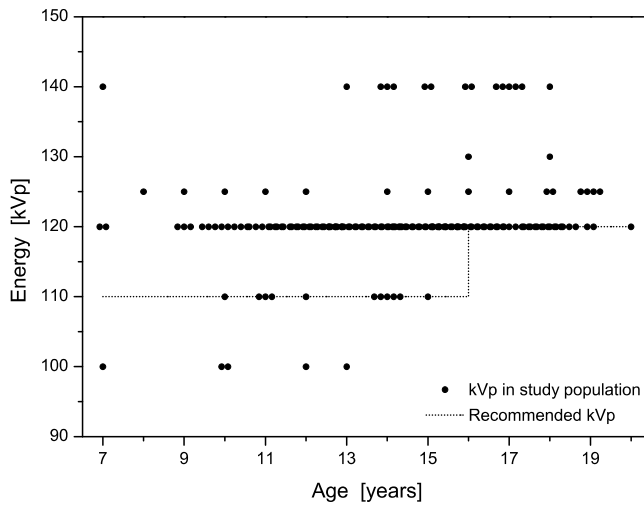


Fig. 17

Selected energies from 100–140 kV for the 169 PA chest tomosynthesis examinations in the study, compared with the recommended tube voltage in the local protocol during the study period. In 125 of the examinations (74%) a higher tube voltage than recommended was used. In 33 of the examinations (19.5%) the tube voltage was set higher than 120 kV. (*Fig. 2 in Paper V⁽¹⁰⁵⁾, reprinted with permission.*)

Mean tube load for tomosynthesis scout acquisition in this study was for the 169 PA examinations 1.30 mAs, and the 17 AP examinations 0.83 mAs.

Phantom examinations

Only minor variations in the registered DAP values were observed when one technician examined the adult phantom using the same settings. Thus, the variability encountered in the DAP values for the patient examinations could not be explained by instabilities of the X-ray system.

Although the same energy of 120 kV was selected by the seven technicians performing the 33 PA tomosynthesis examinations on the adult chest phantom, the registered DAP values varied considerably. For the 33 PA tomosynthesis examinations on the paediatric chest phantom kV settings from 100 to 120 were selected by the technicians. Again registered DAP values varied considerably and increased with increased energy. Consequently, the variability seen in the DAP values for the patient examinations could partly be explained by differences in the examination procedure.

General discussion

In these studies tomosynthesis has been shown to be a valuable tool for monitoring pulmonary cystic fibrosis. Typical imaging findings of this lung disease are well depicted and radiation dose is low, indicating that this imaging modality is promising in the care of these patients, where regular radiological evaluation is important for choice of treatment. A dedicated tomosynthesis scoring system has been designed and validated and may improve diagnostic precision for clinical follow-up of patients as well as for research.

Imaging of pulmonary cystic fibrosis

Chest radiography is the most commonly used imaging modality in the follow-up of patients with cystic fibrosis. It is easily accessible, has low radiation dose and low cost. CT of the chest is generally regarded as the “gold standard”, offering the best combination of high contrast resolution and detailed spatial resolution. The main disadvantage of CT is its high radiation dose⁽⁶⁾. CT protocols with lower dose than conventional are under development⁽¹⁰⁶⁾, but have yet not been implemented in clinical routine. Recently tomosynthesis and MRI⁽⁴³⁻⁴⁶⁾ have emerged as alternatives in the evaluation of pulmonary cystic fibrosis.

An overview of the different imaging modalities ability to depict lung changes typical for cystic fibrosis is presented in Table 2. With radiography small mucus plugs are often not visible. Large mucus plugs can be seen as blurred nodular or cylindrical shadows. Bronchiectasis can be suspected in areas of increased linear markings or blurred cystic lesions. Overinflation, consolidation or atelectasis is, however, generally quite well depicted with radiography. Tomosynthesis and CT provide more detail than radiography, and mucus plugging and bronchiectasis may be clearly visualized. Mucus plugs can be seen as tree-in-bud patterns or as small clustered nodules in the periphery of the lobes, or filling out the bronchi. Bronchiectasis can be differentiated as cylindrical, varicose or cystic. Certain abnormalities, such as air trapping, mosaic perfusion and ground glass opacities can only be evaluated with CT. With MRI⁽⁴³⁻⁴⁶⁾ the spatial resolution is not as high as with tomosynthesis or CT, and bronchiectasis cannot be separated from bronchial wall thickening. Emphysema and air trapping

cannot be evaluated. On the other hand, when MRI is performed using intravenous contrast lung perfusion can be evaluated, which according to preliminary results from on-going studies may allow differentiation between reversible and irreversible lung changes⁽⁴³⁾. It has also been shown that MRI is very sensitive for the detection of mucus plugs, except in small airways⁽⁴⁴⁾.

Owing to the tomographic technique in tomosynthesis adjacent structures such as ribs, bronchi and vessels disturb less. Thereby high contrast changes, such as bronchial wall thickening, mucus plugging and bronchiectasis in the focus plane, are well visualised. In Papers I⁽⁴¹⁾ and II⁽⁴²⁾ tomosynthesis has been shown to be a significantly more sensitive method than chest radiography for the detection of pulmonary cystic fibrosis changes, in accordance with previous results for tomosynthesis in the detection of pulmonary nodules⁽¹¹⁾. Most changes seen with CT could also be evaluated well with tomosynthesis.

Tomosynthesis is performed using the same X-ray system as for radiography and adds only about one minute to the examination time. It is thus quick and easy to perform. Moreover, typical lung changes in cystic fibrosis are well depicted and radiation dose is low^(99, 100). Therefore, it is a competitive alternative for monitoring pulmonary cystic fibrosis. To increase the utility of this new method we developed a scoring system, as there was yet no scoring system published for tomosynthesis when the study started.

Scoring of pulmonary cystic fibrosis

For all imaging modalities described here scoring systems for pulmonary cystic fibrosis have been developed. The purpose of scoring systems is to translate the pathological findings in the images into numbers, in a reproducible and objective way. An evaluation of the general disease progression is of interest, but also the progression of a separate component such as mucus plugging, atelectasis or consolidation. Treatment may then be focused on a specific pathology. Scoring systems are used in the regular follow-up of patients as well as in clinical studies to evaluate the effect of different treatment strategies.

Depending on the imaging modality selected to evaluate pulmonary cystic fibrosis changes, the scored abnormalities and scoring approach differs. In addition, there are large divergences in how the scoring is performed in scoring systems dedicated to the same imaging modality. As shown in Paper III⁽¹⁰⁴⁾ bronchiectasis alone, or in combination with mucus plugging, is considered the most important component of the score in most scoring systems, independent of imaging modality. Some authors have even suggested that selective scoring of these changes might be as sensitive as

more complicated CT scoring systems in observing the course of disease in patients with cystic fibrosis^(63, 76, 107).

Bronchiectasis and mucus plugging are the most specific pulmonary abnormalities of cystic fibrosis^(52, 107) and were therefore given a high weighting in percentage of the total score in the chest tomosynthesis scoring system presented in Paper II⁽⁴²⁾. This scoring system was dedicated to tomosynthesis, adapted from previously reported scoring systems for radiography and CT. As tomosynthesis depicts in particular bronchiectasis and mucus plugging much better than radiography, the scoring systems for radiography where bronchiectasis and mucus plugging are scored together^(51, 56) were not optimal. Moreover, in radiography scoring systems^(50, 51, 55, 56) the components are graded for increasing severity, without clear definitions of the scoring levels, which makes the scoring very subjective. Chest CT score components such as air trapping, mosaic perfusion and thickening of septa cannot be evaluated adequately with tomosynthesis. Furthermore, in most CT scoring systems the lungs are evaluated per lobe or lung segment. These are difficult to distinguish with tomosynthesis⁽¹⁰⁸⁾, therefore the scoring was performed per quadrant. In previous studies the number of abnormal airways found with CT has been shown to correlate with the degree of impairment of pulmonary function⁽³²⁾, and the classification of the type of bronchiectasis (cylindrical, varicose or cystic) has been described as a useful index of disease severity⁽¹⁰⁹⁾. Bronchiectasis was therefore scored for extent as well as for severity.

The Brasfield scoring system⁽⁵¹⁾ for radiography is well established, has previously been validated^(97, 98), and shown to correlate well with tests for lung function. The scoring of tomosynthesis using the new system correlated well with the scoring of radiography using the Brasfield score, but the scores for tomosynthesis showed a greater diversity (Fig. 11) and were generally higher than for radiography (Table 1). Bronchiectasis and mucus plugging are scored together in the Brasfield score as nodular cystic lesions with a maximum score of 4 for both lungs. In the tomosynthesis score these entities are scored separately and the maximum score is 64 for both lungs. This explains the higher diversity of scores using the tomosynthesis score, giving the possibility of earlier detection of disease progression or alteration in lung status compared with using the Brasfield score. For tomosynthesis 17% of the examinations were given a score higher than 50% of the maximum score, compared with 6% for radiography, explained by tomosynthesis' better ability to detect in particular mucus plugging and bronchiectasis. This implies that tomosynthesis, using the presented scoring system, is a more precise and sensitive method to evaluate the dynamics in the disease and the effect of a therapeutic intervention.

Preliminary results from an on-going study in Italy⁽¹¹⁰⁾ (presented as an electronic poster at the European Congress of Radiology 2013) showed high correlation between the scoring of tomosynthesis and CT examinations using a modified

tomosynthesis⁽⁴²⁾ and Brody⁽⁷⁵⁾ score, in 20 adult patients with cystic fibrosis. The scoring system used was similar to the tomosynthesis score presented in Paper II⁽⁴²⁾, with the difference that small and large mucus plugs were not scored separately. The scores for tomosynthesis and CT showed good correlation with forced expiratory volume in 1 s (FEV1). In an on-going study from Gothenburg (presented at the SPIE Medical Imaging Conference in Florida 2013)⁽¹⁰⁸⁾ the Brody score^(75, 111) was used for scoring tomosynthesis and CT. The authors suggested that the Brody score could be adapted to tomosynthesis examinations by excluding the scoring of air trapping, and by performing the scoring per quadrant instead of per lobe. As the lungs in addition are scored for ground glass opacities in the Brody system, this component should also be excluded in a modification of the score, as it cannot be evaluated with tomosynthesis.

The observer agreements for the tomosynthesis score presented in Paper II⁽⁴²⁾ were almost perfect for the total scores and generally substantial to almost perfect for subscores, when validated by three independent observers. However, as the observers all had participated in the development of the system and were familiar with the scoring procedure, interobserver agreements might be lower for other users. The purpose of the scoring sheet and reference PDF (which was included in the online publication) was to provide clear definitions and examples of each scoring level, to reduce interobserver variability. The tomosynthesis score is also suitable for CT, but could be modified to include the scoring of air trapping, which may be an important finding in pulmonary cystic fibrosis as it according to some authors reflects small airway disease in early cystic fibrosis^(107, 112).

The tomosynthesis cystic fibrosis scoring system proved to be robust and is intended for regular follow-up as well as for research. The scoring system can also be used for scoring CT examinations, thus enabling a comparison of the advantages and disadvantages of the two methods in the evaluation of pulmonary cystic fibrosis. It is well known that the dose from paediatric chest CT is high^(6, 113), and previous studies have reported that the dose from chest tomosynthesis in adults is low^(99, 100). It was therefore important to determine the effective dose from chest tomosynthesis also for children.

Effective dose from chest tomosynthesis

Conversion factors between DAP and effective dose are used to estimate the radiation dose from a radiographic examination. As previously shown by Svalkvist *et al.* the conversion factors decrease with increasing weight or BMI, and increase with increasing tube energy⁽⁹²⁾. Consequently, the conversion factors determined for paediatric chest tomosynthesis in Paper IV⁽¹⁰²⁾ were considerably higher than those

previously reported for adults⁽⁹⁹⁾, especially for young children and at high energy settings. With the same energy settings, the conversion factors were significantly higher for examinations performed AP compared with PA, which previously also has been shown by Tapiovaara *et al.*⁽⁸⁹⁾. An increase in Cu filtration also resulted in higher conversion factors, explained by the absorption of more low-energy X-ray photons thus increasing the mean energy of the radiation beam. As the maximum energy does not increase, the effect of Cu filtration on the conversion factors is less marked than that for increased energy.

The significantly higher conversion factors for chest tomosynthesis in young children than reported for adults imply that children receive higher effective doses from ionizing radiation than previously thought. In Study V⁽¹⁰⁵⁾ the mean paediatric effective dose from chest tomosynthesis calculated using the conversion factor of 0.26 mSv/ Gy cm² ⁽⁹⁹⁾ was 0.11 mSv, which is comparable to the effective dose of 0.12–0.13 mSv reported for adults^(99, 100). When using the conversion factors corrected for sex, age and energy (from Paper IV⁽¹⁰²⁾) the mean paediatric effective dose was 0.17 mSv. These conversion factors are specific for each sex, age and energy combination. As a simplification three age dependent conversion factors were proposed for PA chest tomosynthesis in Paper IV⁽¹⁰²⁾: 0.6 (8–10 y), 0.4 (11–14 y) and 0.3 mSv/ Gy cm² (15–19 y), independent of sex and energy setting. Using these simplified conversion factors the calculated mean paediatric effective dose was 0.15 mSv. The difference of 0.02 mSv is mainly explained by the high energies used for many of the paediatric examinations in the study, resulting in higher conversion factors when using the conversion factors corrected for sex, age and energy.

Children under 12 years of age examined AP had been judged to cooperate less well and often the collimation was wider, to compensate for movement. For AP exposures the DAP values, as well as the sex, age and energy corrected conversion factors from Paper IV⁽¹⁰²⁾, were considerably higher. The mean calculated effective dose was 0.58 mSv, which is approximately three times higher than for PA exposures. Hence, AP examinations should be avoided, as the patient is positioned closer to the radiation source and sensitive breast tissue is directly exposed.

The dose from chest tomosynthesis may be unnecessarily high for many children and small patients⁽⁹⁹⁾. The tube load for the tomosynthesis acquisition is in most cases determined by the minimum dose limit of 0.25 mAs per projection and not the dose ratio (which is calculated by multiplying the mAs of the scout image with 10, then distributing the tube load over the 60 projections). When the tube load of the scout image is less than 1.5 mAs, the tube load for each tomosynthesis projection will always be 0.25 mAs. The mean tube load for the tomosynthesis scout acquisition was 1.30 mAs for PA and 0.83 mAs for AP examinations in Study V⁽¹⁰⁵⁾. At high-energy settings this is even a bigger problem, as the effective dose will increase with increasing tube energy when tube load is constant. The tube voltage for the patient

examinations in Study V⁽¹⁰⁵⁾ was in many cases higher than recommended in the protocol during the study period, with a mean tube voltage of 120 kV; and in 19.5% a setting of more than 120 kV was used. Therefore the mean effective dose would have been lower if the technicians had adhered to the protocol. The current recommendation for PA chest tomosynthesis by the manufacturer of the tomosynthesis system at our department is 120 kV for all patients, and might be too high for small patients. Lower tube energy settings than currently often used could be beneficial for children and small patients, as the effective dose would be reduced. Phantom studies to determine the image quality with lower energy settings than 120 kV are planned.

Recently reported mean effective doses from chest CT⁽⁶⁾ were 5.3, 7.5 and 6.4 mSv for children aged below 5, 5–9 and 10–15 years, respectively. In 3–8 % of the CT scans the effective dose was 20 mSv or higher. According to the same report, one radiation-induced solid cancer is expected to develop from every 330–480 chest CT examination in girls. In the US 4 million paediatric CT scans are performed each year, which are projected to cause 4870 future cancers⁽⁶⁾. The mean paediatric effective dose of 0.17 mSv from posteroanterior chest tomosynthesis corresponds to only about 1/40 of the dose from chest CT and approximately 1/5 of the dose from natural background radiation in Sweden, which is estimated to be 1 mSv⁽¹⁰⁾. The effective dose for chest radiography (PA and lateral study) has recently been reported to 0.09–0.1 mSv for adults⁽⁸⁾.

Consequently, the dose from chest tomosynthesis is low. The additional dose from chest tomosynthesis compared with radiography is negligible. As tomosynthesis in addition provides more information, it should be used instead of radiography in the follow-up of patients with cystic fibrosis, when possible. The effective dose from one paediatric chest CT corresponds to approximately 40 tomosynthesis examinations⁽⁶⁾. Therefore, tomosynthesis should also be considered as a low-dose alternative to CT, as most issues can be solved using tomosynthesis.

The role of tomosynthesis in the monitoring of cystic fibrosis

When considering which imaging modality to select to follow disease progression in cystic fibrosis the modality's ability to depict changes specific for pulmonary cystic fibrosis is important (Table 2). However, also other aspects are important such as cost effectiveness, the prerequisites for achieving high patient compliance and, not least, radiation dose (Table 3).

In many countries the cost of an examination is a vital issue, especially if patients are charged directly. Furthermore, a low-dose imaging strategy is important in the care of patients with cystic fibrosis, as most patients will be examined many times during their lifetime. This is particularly of concern for young patients, who are more sensitive to ionizing radiation exposure and have a longer presumed length of life compared with adults^(2, 3, 7).

Table 3.

A comparison of the four different radiologic modalities regarding cost; need for anaesthesia in young children; detail of information provided by the imaging modality; simplicity of the examination procedure; and radiation dose. The approximate cost for each modality, derived from the price list of Skåne Regional Council, Sweden, was compared with the cost of a frontal and lateral radiograph, which was given the factor 1. (Adapted from Table 1 in Paper III⁽¹⁰⁴⁾.)

	Radiography	Tomosynthesis	CT	MRI
Cost, compared with radiography	1	1.1	5.5	10.7
Anaesthesia required for young children	No	Yes	Yes ^a	Yes
Detail of information	Low	Medium	High	Medium
Quick and easy to perform	Yes	Yes	Yes ^a	No
Mean effective dose (mSv)	0.09–0.1 ^b	0.12–0.13 (adults) 0.17 (children) ^c	5.3–7.5 ^d	0

^a Depending on CT system used

^b Reported for adults⁽⁸⁾

^c Reported for adults^(99, 100) and children (Paper V⁽¹⁰⁵⁾)

^d Mean effective dose from paediatric chest CT scans according to a recent study by Miglioretti *et al.*⁽⁶⁾

As tomosynthesis provides more information than radiography at a low dose and cost, it has at our hospital replaced radiography in the follow-up of most of these patients. Mucus plugging and bronchiectasis, which are important findings in cystic fibrosis, can be missed when solely relying on chest radiography. The detection of e.g. mucus plugging with tomosynthesis may lead to intensified physiotherapy and medical therapy. The method is, however, very sensitive to movements of the diaphragm and sometimes structures may be blurred and therefore difficult to evaluate, particularly in the lower lobes. Therefore, it is required that patients hold their breath for 10 s during the tomosynthesis examination, which limits its use in young children and in patients with severely impaired lung function.

At our department, chest CT examinations in cystic fibrosis are only performed in special cases, as the radiation dose⁽⁶⁾ as well as the cost for CT is high compared with radiography (Table 3). Advancements in technology are expected to reduce the radiation dose from CT, which probably will increase the usage of CT for these patients in the future. MRI cannot be performed in young children without anaesthesia, is expensive, and the access to MRI is limited in many hospitals. However, as MRI is performed without radiation it may still be an alternative to CT.

All imaging modalities for cystic fibrosis have their advantages and disadvantages. However, tomosynthesis appears to have the best combination of high image detail, quick acquisition, and low dose. To further determine the roles of tomosynthesis and CT in the monitoring of pulmonary cystic fibrosis, there is an on-going study at our department where patients who are examined with chest CT for clinical reasons also will be examined with tomosynthesis. The purpose of this study is to compare advantages and disadvantages of the two methods. We have also initiated a study in which the tomosynthesis scoring system will be used to evaluate the effect of physiotherapy and medication on patients with an exacerbation of cystic fibrosis lung disease.

Conclusions

Typical imaging findings of pulmonary cystic fibrosis are much better visualised with tomosynthesis compared with radiography. Most pulmonary changes depicted with computed tomography can also be evaluated well with tomosynthesis. The dedicated tomosynthesis scoring system was validated and proved to be robust, and may improve diagnostic precision for clinical follow-up of patients as well as for research. Bronchiectasis and mucus plugging are the most specific pulmonary changes of cystic fibrosis, and were in the majority of reviewed radiological scoring systems considered the most important scoring components.

Conversion factors determined for paediatric chest tomosynthesis were considerably higher for young children than previously reported for adults. With increasing tube energy and filtration the conversion factor increased. The mean paediatric effective dose from posteroanterior chest tomosynthesis was 0.17 mSv, which is about 40 times less than recently reported effective doses from paediatric chest computed tomography. Using the previously reported conversion factor for adults the paediatric effective dose was estimated to 0.11 mSv. Consequently, when using conversion factors not adapted to children for paediatric examinations, the radiation dose may be underestimated. Anteroposterior exposures should be avoided, as the effective dose is approximately three times higher than for posteroanterior exposures. Lower tube energy settings than currently often used could be beneficial for children and small patients, as the effective dose would be reduced.

At our department tomosynthesis has to a great extent replaced radiography in the follow-up of pulmonary cystic fibrosis, and computed tomography is only performed in selected cases. Further studies are planned to determine the roles of tomosynthesis and computed tomography in the monitoring of cystic fibrosis lung disease.

References

1. European Commission (1996). European guidelines on quality criteria for diagnostic radiographic images in paediatrics. ECEUR 16261. ISBN 92-827-7843-6
2. Brenner DJ, Hall EJ (2007) Computed tomography—an increasing source of radiation exposure. *N Engl J Med* 357:2277–2284
3. Strauss KJ, Goske MJ, Kaste SC et al. (2010) Image gently: ten steps you can take to optimize image quality and lower CT dose for pediatric patients. *AJR Am J Roentgenol* 194:868–873
4. Swedish National Board of Health and Welfare (Socialstyrelsen) (2013) Ovanliga diagnoser, cystisk fibros. <http://www.socialstyrelsen.se/ovanligadiagnoser/cystiskfibros>. Accessed 18 September 2013
5. ICRP (2007). The 2007 Recommendations of the International Commission on Radiological Protection. ICRP publication 103. Pergamon Press
6. Miglioretti DL, Johnson E, Williams A et al. (2013) The use of computed tomography in pediatrics and the associated radiation exposure and estimated cancer risk. *JAMA Pediatr* 167(8):700–707
7. Pearce MS, Salotti JA, Little MP et al. (2012) Radiation exposure from CT scans in childhood and subsequent risk of leukaemia and brain tumours: a retrospective cohort study. *The Lancet* 380:499–505
8. Mettler FA, Bhargavan M, Faulkner K et al. (2009) Radiologic and nuclear medicine studies in the United States and worldwide: frequency, radiation dose, and comparison with other radiation sources–1950–2007. *Radiology* 253:520–531
9. Børretzen I, Lysdahl KB, Olerud HM (2007) Diagnostic radiology in Norway—trends in examination frequency and collective effective dose. *Radiat Prot Dosim* 124:339–347

10. Swedish Radiation Protection Authority (Strålsäkerhetsmyndigheten) (2013) Frågor och svar om strålning. <http://www.stralsakerhetsmyndigheten.se/om-myndigheten/aktuellt---bilagor/fragor-och-svar-om-stralning/>. Accessed 26 September 2013
11. Vikgren J, Zachrisson S, Svalkvist A et al. (2008) Comparison of chest tomosynthesis and chest radiography for detection of pulmonary nodules: human observer study of clinical cases1. *Radiology* 249:1034-1041
12. Zachrisson S, Vikgren J, Svalkvist A et al. (2009) Effect of Clinical Experience of Chest Tomosynthesis on Detection of Pulmonary Nodules. *Acta Radiol* 50:884-891
13. Kim E, Chung M, Lee H et al. (2010) Pulmonary mycobacterial disease: diagnostic performance of low-dose digital tomosynthesis as compared with chest radiography1. *Radiology* 257:269-277
14. Mermuys K, De Geeter F, Bacher K et al. (2010) Digital tomosynthesis in the detection of urolithiasis: diagnostic performance and dosimetry compared with digital radiography with MDCT as the reference standard. *AJR Am J Roentgenol* 195:161-167
15. Wells I, Raju V, Rowberry B et al. (2011) Digital tomosynthesis—a new lease of life for the intravenous urogram? *Br J Radiol* 84:464-468
16. Mermuys K, Vanslambrouck K, Goubau J et al. (2008) Use of digital tomosynthesis: case report of a suspected scaphoid fracture and technique. *Skel Radiol* 37:569-572
17. Geijer M, Börjesson AM, Göthlin JH (2011) Clinical utility of tomosynthesis in suspected scaphoid fracture. A pilot study. *Skelet Radiol* 40:863-867
18. Andersen DH (1938) Cystic fibrosis of the pancreas and its relation to celiac disease. *Am J Dis Child* 56:344-399
19. S Brown, Balfour-Lynn IM (2009) Cystic Fibrosis. In: *Pediatric Thoracic Surgery*. Springer-Verlag London Limited. DOI: 10.1007/b136543_35
20. Quinton PM (1983) Chloride impermeability in cystic fibrosis. *Nature* 301:421-422
21. Riordan J, Rommens J, Kerem B, et al. (1989) Identification of the cystic fibrosis gene: cloning and characterization of complementary DNA. *Science* 245:1066-1073
22. Dinwiddie R (2000) Pathogenesis of lung disease in cystic fibrosis. *Respiration* 67:3-8

23. Cole P (1997) The damaging role of bacteria in chronic lung infection. *J Antimicrob Chemoth* 40:S5–S10
24. Matsui H, Grubb BR, Tarran R et al. (1998) Evidence for periciliary liquid layer depletion, not abnormal ion composition, in the pathogenesis of cystic fibrosis airways disease. *Cell* 95:1005–1015
25. Chmiel J, Berger M, Konstan M (2002) The role of inflammation in the pathophysiology of CF lung disease. *Clin Rev Allerg Immun* 23:5–27
26. Boucher R (1998) ASL in normal and CF subjects is isotonic: Evidence for the isotonic volume absorption/mucus clearance hypothesis for the pathogenesis of early CF lung disease. *Pediatr Pulmonol Suppl* 17:132
27. Sturgess J, Imrie J (1982) Quantitative evaluation of the development of tracheal submucosal glands in infants with cystic fibrosis and control infants. *Am J Pathol* 106:303–311
28. Davis PB (2006) Cystic fibrosis since 1938. *Am J Resp Crit Care Med* 173:475–482
29. Cole P, Wilson R (1989) Host-microbial interrelationships in respiratory infection. *Chest* 95:217S–221S
30. Konstan MW, Berger M (1997) Current understanding of the inflammatory process in cystic fibrosis: onset and etiology. *Pediatr Pulm* 24:137–142
31. Reid L (1950) Reduction in bronchial subdivision in bronchiectasis. *Thorax* 5:233–247
32. Barker AF (2002) Bronchiectasis. *N Engl J Med* 346:1383–1393
33. Farrell PM, Rosenstein BJ, White TB et al. (2008) Guidelines for diagnosis of cystic fibrosis in newborns through older adults: Cystic Fibrosis Foundation consensus report. *J Pediatr* 153:S4–S14
34. Scotet V, De Braekeleer M, Audrezet M-P et al. (2002) Prenatal detection of cystic fibrosis by ultrasonography: a retrospective study of more than 346 000 pregnancies. *J Med Genet* 39:443–448
35. Farrell PM, Li Z, Kosorok MR et al. (2003) Bronchopulmonary disease in children with cystic fibrosis after early or delayed diagnosis. *Am J Resp Crit Care Med* 168:1100–1108
36. Rowe SM, Clancy JP (2006) Advances in cystic fibrosis therapies. *Curr Opin Pediatr* 18:604–613
37. FitzSimmons SC (1993) The changing epidemiology of cystic fibrosis. *J Pediatr* 122:1–9

38. Aziz ZA, Davies JC, Alton EW et al. (2007) Computed tomography and cystic fibrosis: promises and problems. *Thorax* 62:181–186
39. Cooper P, MacLean J (2006) High-resolution computed tomography (HRCT) should not be considered as a routine assessment method in cystic fibrosis lung disease. *Paediatr Respir Rev* 7:197–201
40. Tiddens HAWM (2006) Chest computed tomography scans should be considered as a routine investigation in cystic fibrosis. *Paediatr Respir Rev* 7:202–208
41. Vult von Steyern K, Björkman-Burtscher I, Geijer M (2012) Tomosynthesis in pulmonary cystic fibrosis with comparison to radiography and computed tomography: a pictorial review. *Insights Imaging* 3:81–89
42. Vult von Steyern K, Björkman-Burtscher IM, Höglund P et al. (2012) Description and validation of a scoring system for tomosynthesis in pulmonary cystic fibrosis. *Eur Radiol* 22:2718–2728
43. Eichinger M, Puderbach M, Fink C et al. (2006) Contrast-enhanced 3D MRI of lung perfusion in children with cystic fibrosis-initial results. *Eur Radiol* 16:2147–2152
44. Puderbach M, Eichinger M, Gahr J, et al. (2007) Proton MRI appearance of cystic fibrosis: comparison to CT. *Eur Radiol* 17:716–724
45. Puderbach M, Eichinger M, Haeselbarth J et al. (2007) Assessment of morphological MRI for pulmonary changes in cystic fibrosis (CF) patients: comparison to thin-section CT and chest x-ray. *Investigative radiology* 42:715–725
46. Eichinger M, Optazait D-E, Kopp-Schneider A et al. (2012) Morphologic and functional scoring of cystic fibrosis lung disease using MRI. *European journal of radiology* 81:1321–1329
47. Shwachman H, Kulczycki L (1958) Long-term study of one hundred five patients with cystic fibrosis: studies made over a five-to fourteen-year period. *AMA J Dis Child* 96:6–15
48. Taussig L, Kattwinkel J, Friedewald W et al. (1973) A new prognostic score and clinical evaluation system for cystic fibrosis. *J Pediatr* 82:380–390
49. Holzer F, Olinsky A, Phelan P (1981) Variability of airways hyper-reactivity and allergy in cystic fibrosis. *Arch Dis Child* 56:455–459
50. Chrispin A, Norman A (1974) The systematic evaluation of the chest radiograph in cystic fibrosis. *Pediatr Radiol* 2:101–105

51. Brasfield D, Hicks G, Soong S et al. (1979) The chest roentgenogram in cystic fibrosis: a new scoring system. *Pediatrics* 63:24–29
52. Van der Put J, Meradji M, Danoesastro D et al. (1982) Chest radiographs in cystic fibrosis. A follow-up study with application of a quantitative system. *Pediatr Radiol* 12:57–61
53. Carty H (1987) The chest radiograph in cystic fibrosis in children and the role of other radiological techniques. *J R Soc Med* 80:38–46
54. O'Laoide R, Fahy J, Coffey M et al. (1991) A chest radiograph scoring system in adult cystic fibrosis: Correlation with pulmonary function. *Clin Radiol* 43:308–310
55. Weatherly M, Palmer C, Peters M et al. (1993) Wisconsin cystic fibrosis chest radiograph scoring system. *Pediatrics* 91:488–495
56. Conway S, Pond M, Bowler I et al. (1994) The chest radiograph in cystic fibrosis: a new scoring system compared with the Chrispin-Norman and Brasfield scores. *Thorax* 49:860–862
57. Koscik R, Kosorok M, Farrell P et al. (2000) Wisconsin cystic fibrosis chest radiograph scoring system: validation and standardization for application to longitudinal studies. *Pediatr Pulmonol* 29:457–467
58. Benden C, Wallis C, Owens C et al. (2005) The Chrispin-Norman score in cystic fibrosis: doing away with the lateral view. *Eur Respir J* 26:894–897
59. Terheggen-Lagro S, Truijens N, van Poppel et al. (2003) Correlation of six different cystic fibrosis chest radiograph scoring systems with clinical parameters. *Pediatric pulmonology* 35:441–445
60. Kerem E, Conway S, Elborn S et al. (2005) Standards of care for patients with cystic fibrosis: a European consensus. *J Cyst Fibros* 4:7–26
61. Hounsfield GN (1973) Computerized transverse axial scanning (tomography): Part 1. Description of system. *Brit J Radiol* 46:1016–1022
62. Cormack AM (1964) Representation of a function by its line integrals with some radiological applications. *J App Phys* 35:2908–2913
63. Nathanson I, Conboy K, Murphy S et al. (1991) Ultrafast computerized tomography of the chest in cystic fibrosis: a new scoring system. *Pediatr Pulmonol* 11:81–86
64. Bhalla M, Turcios N, Aponte V et al. (1991) Cystic fibrosis: scoring system with thin-section CT. *Radiology* 179:783–788

65. Stiglbauer R, Schurawitzki H, Eichler I et al. (1992) High resolution CT in children with cystic fibrosis. *Acta Radiol* 33:548–553
66. Maffessanti M, Candusso M, Brizzi F et al. (1996) Cystic fibrosis in children: HRCT findings and distribution of disease. *J Thorac Imag* 11:27–38
67. Donnelly L, Gelfand MJ, Brody AS (1997) Comparison between morphologic changes seen on high-resolution CT and regional pulmonary perfusion seen on SPECT in patients with cystic fibrosis. *Pediatr Radiol* 27:920–925
68. Shah R, Sexauer W, Ostrum B et al. (1997) High-resolution CT in the acute exacerbation of cystic fibrosis: evaluation of acute findings, reversibility of those findings, and clinical correlation. *AJR Am J Roentgenol* 169:375–380
69. Santamaria F, Grillo G, Guidi G et al. (1998) Cystic fibrosis: when should high-resolution computed tomography of the chest be obtained? *Pediatrics* 101:908–913
70. Brody A, Molina P, Klein J et al. (1999) High-resolution computed tomography of the chest in children with cystic fibrosis: support for use as an outcome surrogate. *Pediatr Radiol* 29:731–735
71. Helbich T, Heinz-Peer G, Eichler I et al. (1999) Cystic fibrosis: CT assessment of lung involvement in children and adults. *Radiology* 213:537–544
72. Castile R, Hayes J, Flucke R et al. (2000) Correlation of structural and functional abnormalities in the lungs of infants with cystic fibrosis (Abstract). *Pediatric Pulmonology* 20:A427
73. Robinson T, Leung A, Northway W et al. (2001) Spirometer-triggered high-resolution computed tomography and pulmonary function measurements during an acute exacerbation in patients with cystic fibrosis. *J Pediatr* 138:553–559
74. Oikonomou A, Manavis J, Karagianni P et al. (2002) Loss of FEV1 in cystic fibrosis: correlation with HRCT features. *Eur Radiol* 12:2229–2235
75. Brody A, Klein J, Molina P et al. (2004) High-resolution computed tomography in young patients with cystic fibrosis: distribution of abnormalities and correlation with pulmonary function tests. *J Pediatr* 145:32–38
76. Oikonomou A, Tsanakas J, Hatziagorou E et al. (2008) High resolution computed tomography of the chest in cystic fibrosis (CF): is simplification of scoring systems feasible? *Eur Radiol* 18:538–547

77. Grant DG (1972) Tomosynthesis: a three-dimensional radiographic imaging technique. *Biomed Eng*, 19:20–28
78. Radon J (1917) Über die bestimmung von funktionen durch ihre integralwerte längs gewisser mannigfaltigkeiten. *Ber Verh Sächs Akad Wiss Leipzig, Math. Nat. kl.* 69:262–277
79. Ziedses des Plantes BG (1932) Eine neue methode zur differenzierung in der rontgenographie (planigraphies). *Acta Radiologica* 13:182–192
80. Dobbins JT, Godfrey DJ (2003) Digital x-ray tomosynthesis: current state of the art and clinical potential *Phys Med Biol* 48:R65–R106
81. Dobbins JT, McAdams HP (2009) Chest tomosynthesis: technical principles and clinical update. *Eur J Radiol* 72:244–251
82. Frieben H (1902) Demonstration eines cancroïd des rechten handrückens, das sich nach langdauernder einwirkung von röntgenstrahlen entwickelt hatte. *Fortschr Roentgenstr* 6:106–111
83. Henshaw PS, Hawkins JW, Meyer HL et al. (1944) Incidence of leukemia in physicians. *J Natl Cancer I* 4:339–346
84. Ulrich H (1946) The incidence of leukemia in radiologists. *N Engl J Med* 234:45–46
85. Lewis EB (1957) Leukemia and ionizing radiation. *Science* 125:965–972
86. Pierce DA, Shimizu Y, Preston DL et al. (1996) Studies of the mortality of atomic bomb survivors. Report 12, Part I. Cancer: 1950-1990. *Radiat Res* 146:1–27
87. Stecker MS, Balter S, Towbin RB et al. (2009) Guidelines for patient radiation dose management. *J Vasc Interv Radiol* 20:S263-S273
88. Nickoloff EL, Lu ZF, Dutta AK et al. (2008) Radiation Dose Descriptors: BERT, COD, DAP, and Other Strange Creatures1. *Radiographics* 28:1439–1450
89. Tapiovaara M, Siiskonen T (2008) PCXMC—a Monte Carlo program for calculating patient doses in medical x-ray examinations (2nd edition). STUK-A231. STUK
90. Cristy M (1980) Mathematical phantoms representing children of various ages for use in estimates of internal dose. Oak Ridge National Laboratory NUREG.cr-1159, ORNL/NUREG/TM-367
91. ICRP (1991) 1990 Recommendations of the International Commission on Radiological Protection. ICRP 60. Pergamon Press

92. Svalkvist A, Månsson LG, Båth M (2010) Monte Carlo simulations of the dosimetry of chest tomosynthesis. *Radiat Prot Dosim* 139:144–152
93. Landis JR, Koch GG (1977) The measurement of observer agreement for categorical data. *Biometrics* 33:159–174
94. Svensson E, Holm S (1994) Separation of systematic and random differences in ordinal rating scales. *Stat Med* 13:2437–2453
95. Svensson E, Starmark JE, Ekholm S et al. (1996) Analysis of interobserver disagreement in the assessment of subarachnoid blood and acute hydrocephalus on CT scans. *Neurol Res* 18:487–494
96. Thomson Reuters (2013) Web of Science. Available via <http://thomsonreuters.com/web-of-science/>
97. Wong E, Regnis J, Shnier R et al. (1993) The relationship between tests of lung function and three chest radiological scoring systems in patients with cystic fibrosis. *Australas Radiol* 37:265–269
98. Sawyer S, Carlin J, DeCampo M et al. (1994) Critical evaluation of three chest radiograph scores in cystic fibrosis. *Thorax* 49:863–866
99. Båth M, Svalkvist A, von Wrangel A et al. (2010) Effective dose to patients from chest examinations with tomosynthesis. *Radiat Prot Dosim* 139:153–158
100. Sabol JM (2009) A Monte Carlo estimation of effective dose in chest tomosynthesis. *Med Phys* 36:5480–5487
101. Werner B, Bodin L (2006) Growth from birth to age 19 for children in Sweden born in 1981: Descriptive values. *Acta Paediatr* 95:600–613
102. Vult von Steyern K, Björkman-Burtscher IM, Geijer M et al. (2013) Conversion factors for estimation of effective dose in paediatric chest tomosynthesis. *Radiat Prot Dosim* doi:10.1093/rpd/nct142
103. Saxeböl G, Olerud HM (1996) NRPA, Nordic guidance levels for patient doses in diagnostic radiology. Report on Nordic Radiation Protection Co-operation, No. 5. Norwegian Radiation Protection Authority ISBN 0804-5038
104. Vult von Steyern K, Björkman-Burtscher IM, Geijer M (2013). Radiography, tomosynthesis, CT and MRI in the evaluation of pulmonary cystic fibrosis: an untangling review of the multitude of scoring systems. *Insights Imaging* doi:10.1007/s13244-013-0288-y

105. Vult von Steyern K, Björkman-Burtscher IM, Weber L et al (2013) Effective dose from chest tomosynthesis in children. *Radiat Prot Dosim* doi:10.1093/rpd/nct224
106. Loeve M, Lequin MH, de Bruijne M et al. (2009) Cystic fibrosis: are volumetric ultra-low-dose expiratory CT scans sufficient for monitoring related lung disease? *Radiology* 253:223–229
107. de Jong P, Tiddens H (2007) Cystic fibrosis specific computed tomography scoring. *Proc Am Thorac Soc* 4:338–342
108. Söderman C, Johnsson Å, Vikgren J et al. (2013) Application of a computed tomography based cystic fibrosis scoring system to chest tomosynthesis. *Medical imaging 2013: Image perception, observer performance, and technology assessment*, 86731H, Florida, USA doi:10.1117/12.2006761
109. Lynch DA, Newell J, Hale V et al. (1999) Correlation of CT findings with clinical evaluations in 261 patients with symptomatic bronchiectasis. *AJR Am J Roentgenol* 173:53–58
110. Nespoli P, Parlatano D, L. Cardinale et al. (2013) Pulmonary tomosynthesis in adult with Cystic Fibrosis: our preliminary experience. *ECR 2013 Scientific Exhibit*, doi:10.1594/ecr2013/C-2204
111. Brody AS, Kosorok MR, Li Z et al. (2006) Reproducibility of a scoring system for computed tomography scanning in cystic fibrosis. *J Thorac Imag* 21:14–21
112. Bonnel AS, Song SM, Kesavarju K et al. (2004) Quantitative air-trapping analysis in children with mild cystic fibrosis lung disease. *Pediatr Pulmonol* 38:396–405
113. Donadieu J, Roudier C, Saguintaah M et al. (2007) Estimation of the radiation dose from thoracic CT scans in a cystic fibrosis population. *Chest* 132:1233–1238